M 2014

U.PORTO
FEUP FACULDADE DE ENGENHARIA
UNIVERSIDADE DO PORTO

Establishment of a cellularized artificial model of the gastric wall

JOÃO MIGUEL QUINTAS COENTRO

DISSERTAÇÃO DE MESTRADO APRESENTADA
À FACULDADE DE ENGENHARIA DA UNIVERSIDADE DO PORTO EM BIOENGENHARIA

- This page was intentionally left blank. -

Universidade do Porto
FEUP Faculdade de Engenharia

U.PORTO
INSTITUTO DE CIÊNCIAS BIOMÉDICAS ABEL SALAZAR
UNIVERSIDADE DO PORTO

Faculdade de Engenharia da Universidade do Porto

Instituto de Ciências Biomédicas Abel Salazar

Establishment of a cellularized artificial model of the gastric wall

João Miguel Quintas Coentro

Master Thesis
Submitted in partial fulfilment
of the requirements for the Degree of
Master of Science in Bioengineering,
at the Faculdade de Engenharia da Universidade do Porto
and Instituto de Ciências Biomédicas Abel Salazar

Supervisor: Pedro Granja
Co-Supervisor: Tiago dos Santos

October 2014

Abstract

Cellular permeation models are tools of the upmost importance when studying the application of new drugs for therapeutic use, since they help predict the physiological effects, as well as the drug absorption rate and metabolism of new molecules, making them an easy, reproducible, ethical and cost-effective method for assessing drug-absorption and toxicity mechanisms [1]. Although some *in vitro* permeation models were already developed for the intestinal, pulmonary, nasal, vaginal, rectal, ocular and skin tissues, including triple co-culture *in vitro* models of the intestine [2-4], surprisingly few established *in vitro* permeation models of the gastric wall exist, especially due to the difficulties in maintaining primary gastric cultures [5], and among these only simple co-cultures were used. Therefore, the development of a triple co-culture model of permeation for the stomach is of paramount importance for the evaluation of new therapeutic agents.

The main objective of this project was to optimize and establish a triple co-culture *in vitro* cellular model of the gastric wall to replicate its functional and morphological architecture with application in permeability, toxicity and functional assays. In order to accomplish this, a triple co-culture model of the stomach was established, including fibroblasts, macrophages and epithelial cells. The integrity of the membrane formed was assessed over time, the permeability of the created barrier model to the passage of substances was quantified and the model was further morphologically and structurally characterized.

NST20 fibroblasts were cultured upon transwell membranes, which were then either coated with Matrigel™ or PuraMatrix™, and MKN28 epithelial cells were seeded on top of this coating, to mimic both the mucosa's epithelium and *lamina propria*. Permeability assays using FITC-dextran were used to assess the model's integrity. The optimal cell densities to build the model were determined, namely of 5×10^3 NST20 fibroblasts, 5×10^3 THP-1 derived macrophages and 5×10^4 MKN28 epithelial cells, when cultured in either Matrigel™ or PuraMatrix™. The optimized barrier model yielded moderately high trans-epithelial electric resistance values of about 200 $\Omega.cm^2$, which correlate to a high membrane integrity, and low apparent FITC-dextran permeability (approximately 1×10^{-6}cm/s), as desired. The model was further characterized structurally by fluorescence, confocal and transmission electron microscopy, showing epithelial tight junctions, and the formation of a cohesive, tightly knit epithelium.

The model herein developed constitutes a step forward in the development of *in vitro* model systems of the stomach, by exhibiting rudimentary compositional and functional characteristics of the gastric wall. Considering the present results, the application of the developed model as a cellular *in vitro* permeation model for the gastric wall seems viable, although further optimization and functional and structural characterization is required.

- This page was intentionally left blank. -

Acknowledgments

First and foremost I would like to express my deepest gratitude to my family, namely my parents, for all the support, help, patience and sacrifice during all these years, which made all this possible and my brother, for sharing so much of my interests and always laugh with me at the things that nobody else would.

I also could not have done any of this without my second family, for meeting you was truly one of the best things in my life, and I will always cherish the (more frequent than it should be acceptable) times we were looked sideways for bursting in laughter at the most inappropriate times and subjects.

Secondly, I would like to voice my gratitude to my thesis advisor, Dr. Pedro Granja, for welcoming me in his group and giving me the opportunity to develop my Master's Thesis in a field that I deeply care for, as well as for his optimism and pondered advice.

I also want to extend my sincere gratitude to Dr. Tiago dos Santos, my thesis co-advisor, for all the ever prompt support and advice and also for his welcoming demeanour, which enabled a healthy working environment, as well as a carefree exchange of ideas, essential to scientific growth.

To the friends I grew up with, thank you for all the great moments we shared all these years, for being there when I needed the most and for helping me be the man I am today.

To my friends, with whom I lived, during these 5 years, I could not have asked for better housemates, thank you for all the shared conversations, philosophical debates and constant support.

To the friends I shared, during all of these months, most of my time (and working space) with, thank you for the equilibrated combination of healthy distractions and helpful support.

To all Inebians, for welcoming me as a part of your family (which we truly are) and for always having the time to help a newcomer with a smile.

To Drª. Salette Reis and her group, for the collaboration, while being incredibly helpful.

Finally, to FEUP and ICBAS, for in the end, you were like a second home during these 5 years.

- This page was intentionally left blank. -

Table of Contents

List of Figures

- This page was intentionally left blank. -

Glossary

3D – Three Dimensional

DAPI – 4',6-diamidino – 2 –phenylindole

ECM – Extracellular Matrix

FBS – Fetal Bovine Serum

FITC-dextran – Fluorescein isothiocyanate-dextran

HBSS – Hank's Balanced Saline Solution

IFM – Inverted Fluorescence Microscopy

P/S – Penicillin – Streptomycin

P_{app} – Apparent permeability

PBS – Phosphate Balanced Saline

PDLCL- Poly (D, L-lactide) and ε-caprolactone

PFA – Paraformaldehyde

PGA – Poly glycolic acid

PMA – phorbol- 12 – myristate – 13 – acetate

TEER – Trans-Epithelial Electric Resistance

TEM – Transmission Electron Microscopy

- This page was intentionally left blank. -

Chapter 1

Introduction

1.1. Contextualization

Gastric drug absorption is generally lower than intestinal drug absorption. However, acidic and weak basic drugs can be absorbed in the human stomach through passive diffusion, passive transport (aqueous channel-mediated transport) or active receptor-mediated transport [6]. This can be useful when the therapeutic target is the stomach, since the drug residence time can be greatly increased, thus enhancing the local therapeutic action [7].

In order to assess the application of new drugs for therapeutic use, tools that help predict the physiological effects, as well as the drug absorption rate and metabolism of new molecules are of the utmost importance. Tissue engineering appears as a viable option, since it may provide for a partial replication of the *in vivo* conditions of the human body, namely the stomach. *In vitro* cellular permeation models are an example of such a tool, since they represent an easy, reproducible, ethical and cost-effective method for assessing drug-absorption mechanisms [1].

Despite the obvious applications of an *in vitro* model to study and predict the permeability of the gastric wall to certain drugs, few established *in vitro* permeation models of the gastric mucosa exist, especially due to the difficulties in maintaining primary gastric cultures [5].

Although some *in vitro* permeation models were already developed for the intestinal, pulmonary, nasal, vaginal, rectal, ocular and skin tissues, including triple co-culture *in vitro* models of the intestine [2-4], surprisingly few of these models were created when the stomach is concerned [8], and only simple co-cultures were used. Hence, this is a relatively unexplored field, where there is still much to be done. Therefore, the development of a triple co-culture model of permeation for the stomach proposed here has the potential to be an invaluable tool for the evaluation of new therapeutic agents, with application in the pharmaceutical industry.

1.2. Anatomy and physiology of the stomach

Anatomically speaking, the stomach is divided into five regions: the cardia and gastroesophageal junction, the fundus, the corpus, the antrum and the pylorus (Fig. 1). Functionally speaking, while the fundus and the corpus harbor acid-secreting glands, the

antrum is composed by an alkaline-secreting surface epithelium and endocrine, gastrin-secreting G-cells[9].

The gastric glands, responsible for the secretion of acid, are divided between pepsinogen-secreting chief cells, HCL-secreting parietal cells, mucus neck cells, surface epithelial cells and enterochromaffin-like cells expressing histidine decarboxylase, essential to the production of histamine[10]. These elements are represented in Fig. 2.

In order to protect the stomach from digesting itself, other glands release a thick mucus, mostly formed by mucin, which prevents damage to the stomach epithelium from the acid and pepsin [9].

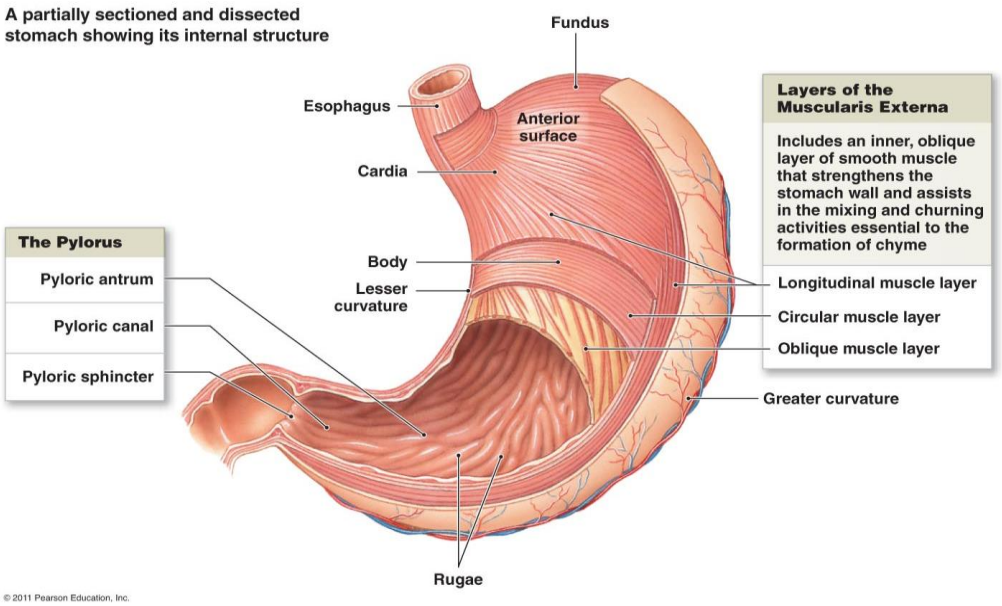

Figure 1 - Anatomy of the stomach, evidencing the different anatomical regions. Source: http://www.highlands.edu/academics/divisions/scipe/biology/faculty/harnden/2122/images/stomachinternal.jpg

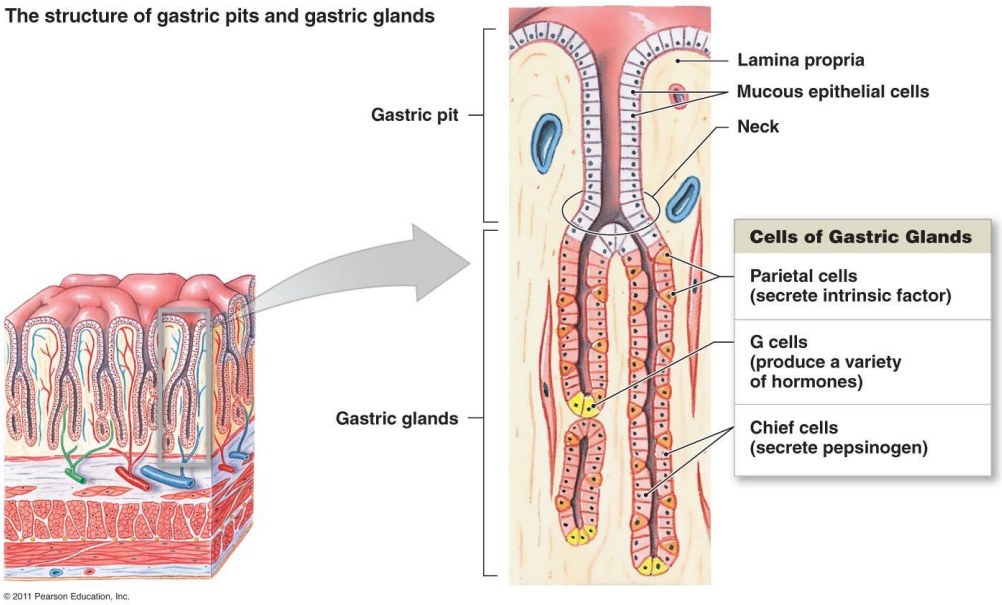

Figure 2 - Gastric glands and gastric pits structure. Source: http://www.highlands.edu/academics/divisions/scipe/biology/faculty/harnden/2122/images/stomachcells.jpg

1.3. Tissue engineering

Tissue engineering is an area based on cell transplantation, materials science and engineering with the purpose of developing biological substitutes that can restore and maintain the normal function of a damaged tissue or organ [11]. Although not among its main targets, tissue engineering can also be applied to the establishment of cellular models that try to replicate the pretended tissues or organs, in order to use them for drug or diagnosis methods testing [12].

Tissue engineering can be divided mainly into two main approaches: the use of acellular scaffolds or scaffolds seeded with cells [11]. For the purpose of this work we will consider mainly the latter, since our goal is to develop a cellular model that mimics the physiological conditions of the stomach.

Besides the already mentioned interest in the development of cellular models, tissue engineering of the stomach is motivated by the need to restore the normal capacity for food intake and digestion after end-stage organ failure and tissue loss or after a gastrectomy (such as in the case of gastric cancer), since the existent alternatives, such as reconstruction of the stomach through jejunal interposition, were shown not to improve the quality of life of the patient, leading to malnutrition, anaemia and weight loss [13-15].

Although many cellular models exist for other tissues, the attempts at modelling the gastric mucosa have been modest, relying mainly on biomechanical *in vitro* systems composed by pumps and different compartments with a simulated gastric fluid [8, 16]. Numerous attempts have been undertaken to establish primary cultures of gastric epithelial cells in several animal models, with only a few being successful [17-19]. This is due to the fact that the stomach comprises many types of cells, including epithelial cells, smooth muscle cells, mesenchymal cells, vessel-forming cells, nerve cells, immune cells and gastric gland cells, with epithelial cells being further divided into at least eleven more different types [20].

As a result, two major problems can be found when trying to culture gastric epithelial cells: i) cell purification - since there are so many different types, it is difficult to obtain a highly purified culture consisting of a single type [14, 21]; ii) and cell differentiation - cells begin to de-differentiate and lose their terminal differentiated characteristics after being seeded [22].

A way to overcome these difficulties consists in using an acellular approach, in which biomaterials can be used to develop new appropriate tissue within the host [14]. The scaffolds developed for that purpose have taken into account the mechanical properties and degradation kinetics [23, 24] and have ranged from collagen sponges reinforced with poly glycolic acid (PGA) [25] to three-layer scaffolds composed of poly(D,L-lactide) and ε-caprolactone, collagen and PGA nonwoven fabrics [26].

Some attempts have included the use of an acellular collagen scaffold reinforced with PGA, which was then covered by a silicone sheet [27] and later poly(D,L-lactide) and ε-caprolactone (PDLCL) instead of the silicon sheet [26]. Although some degree of regeneration of a mucosal and submucosal layer has been reported, with a differentiated epithelium and no anastomotic problems have been reported, the defects ended up shrinking due to inflammation [25, 26].

Alternative approaches have been focused on the use of stomach epithelium organoid units (consisting of epithelium and mesenchyme) to allow epithelial-mesenchymal cell interactions that are essential for survival, morphogenesis, proliferation and differentiation, in order to correctly promote the regenerative capacity of the stomach [13]. In spite of some studies being successful in the formation of tissue engineered stomachs *in vitro* and *in vivo* [13, 28, 29], a complete gastric gland formation, with the presence of mucous, parietal, chief and enteroendocrine cells [8, 30], as well as of repairing lesions in the gastric wall though tissue engineered gastric walls [31], there are still some pressing problems to be resolved, such as being able to combine neomucosa and smooth muscle layer in the same model [25] or

addressing the limitations of *ex vivo* tissue engineering approaches, such as insufficient blood supply [14].

Furthermore, in order to create long-term sustainable tissue engineered stomachs, it is necessary to replicate the parasympathetic innervations, so that these stomachs could have normal functionality and effectiveness, as well as being correctly coordinated by the nervous and endocrine system [14], although simpler configurations would still allow for the restoration of some function and could be applicable in permeation, toxicity or functional assays .

1.4. Cellular permeation models

Cellular models can have various applications, namely in drug development, where they can act as low cost platforms that reproduce the physiological conditions and the various cellular and molecular interactions, making it possible to conduct toxicity and efficacy tests in a low cost model, as well as in determining a formulation strategy, thus reducing the cost of drug testing [12, 32, 33].

Cellular permeation models have been developed for various tissues, including intestinal, nasal mucosa, skin, pulmonary, vaginal, rectal and ocular tissue [32]. It is relevant to understand the variety of strategies used for the various distinct tissues in order to conceive the most adequate strategy to develop a gastric wall model.

1.2.1. Intestinal and colorectal permeation models

Since the oral route is considered the preferred drug route of administration, being easier to administer, more user-friendly and less invasive, the intestinal mucosa is one of the main barriers of drug absorption. Therefore, it is a highly interesting barrier to replicate *in vitro*.

The intestinal mucosa is composed by an epithelial layer, the lamina propria (collagen matrix containing blood and lymphatic vessels) and the muscularis mucosa [32].

Since primary cultures of enterocytes are usually unable to form an organized epithelial monolayer, immortalized cell cultures are usually used instead [34]. One of the most widely used cell models are Caco-2 cell monolayers [35-37], which are derived from a human colorectal carcinoma. These can later be differentiated into mature enterocyte-like cells on a semi-permeable membrane, thus enabling the separation between the apical and basolateral compartments [38].

Besides monolayer cultures, some co-culture models have been investigated in order to more closely represent the heterogeneity of the intestinal epithelium [38]. Some examples include the double co-culture models Caco-2/HT29 cells [36] and the Caco-2/Raji B cells [39] and, recently, the triple co-culture Caco-2/HT29/Raji B cells model, which was claimed as especially suitable to study nanocarrier permeation [3].

Since the epithelial layer at the colorectum shares similarities with the colon-derived cell monolayers, the Caco-2 model is also presented as suitable for the assessment of rectal drug absorption [40], with results showing a good correlation between Caco-2 cell monolayers and excised human colorectal tissues for low molecular weight molecules[35].

1.2.2. Vaginal permeation models

Although different models have been proposed regarding drug permeability trough vaginal administration, the most studied *in vitro* model consists on the harvest of cervical-vaginal cells that are grown on collagen-coated ceramic-based filters and differentiated into multi-

layered stratified squamous epithelium, retaining most of the phenotypical and biologic characteristics of the human cervical-vaginal epithelium [41].

Cervical cell lines, such as the CaSki line can also be an alternative to primary cell cultures, being able to be cultured in mono, bi or tri layers[42] and then used in permeation studies, which have been important in the study of the importance of tight junctions and its modulation on transepithelial electrical resistance (TEER)[43], as well as the modulation of the permeability to pyramine[44].

A commercial model, called EpiVaginal™, based on a 3D culture of non-transformed human vaginal-ectocervical epithelial cells grown on polycarbonate cell culture tissue inserts, also presents a differential multi-layer structure containing non-epithelial elements, such as lamina propria or dendritic cells[45], making it a promising option for permeability studies, with results showing that it is indeed a viable permeation model, since it was possible to provide evidence of increased insulin permeability through reversible disruption of tight junctions by hydrogen peroxide[46]

1.2.3. Respiratory mucosa permeation models

The systemic administration of drugs through inhalation has been gathering increased interest and, as such, makes permeation study models for the respiratory mucosa even more attractive [32].

Although both primary cultures [47] and immortalized cell lines [48] have been used in permeation models, the latter are the most widely used, since primary cell cultures are more expensive, difficult and time consuming to maintain [10].

Regarding bronchial epithelial cell lines, the Calu-3 and 16HBE14o$^-$ cell lines cultivated in monolayers have been used as models for the airway epithelium [48, 49], with studies showing that culture conditions can affect the morphologic characteristics and the TEER of the monolayers, as well as the pattern of drug permeation, although being suitable as a model of the tracheobronchial epithelium[50, 51].

Concerning the alveolar region, A549 cells have been used as a model of absorption [52]. However, due to its incapacity to form tight monolayers, primary cultures of human alveolar epithelial cells (hAEpC) are preferred [53].

Some examples of co-cultures include a 3D triple co-culture monolayer composed by A549 epithelial cells, blood monocyte-derived macrophages and dendritic cells, which resemble the *in vivo* architecture of the human airway epithelial barrier [54], with studies showing the expression of proteins involved in cell-cell interactions and tight junction formation[54], although the presence of macrophages and dendritic cells reduces the integrity of the triple co-culture monolayer[55] and co-cultures of lung epithelial cell lines (NCI-H441) or primary human type II alveolar epithelial cells (HATII) and primary human pulmonary microvascular endothelial cells (hPMEC), which present the morphologic and histological characteristics of the alveolocapilary barrier [56].

Monolayers obtained from primary cultures of human nasal epithelial cells and cell lines such as RPMI 2650 have been extensively used for nasal permeation studies [10, 57, 58].

Co-cultures using a collagen matrix embedded with human nasal fibroblasts covered by a RPMI 2650 epithelial cell layer have also been developed, resembling a non-pseudostratified, non-ciliated epithelium with permeation barrier properties comparable with excised nasal mucosa[58].

1.2.4. Ocular permeation models

Although numerous cell models of the ocular barriers have been established, the human corneal epithelium HCE-T cell model represents a standard tool for drug permeation tests [59].

The IOBA-NHC cell line, a spontaneously immortalized epithelial cell line derived from human conjunctiva, also demonstrated high proliferative capacity *in vitro* and typical epithelial morphology, with some studies showing the viability of this model in the study of transepithelial antigen delivery [60, 61].

Monolayers of immortalized ARPE-19 cell lines have also been applied as a model for the outer blood-retinal barrier, as a model for targeted drug delivery systems[62], since they replicate the morphology, the expression of retina-specific markers and the barrier properties of the retina[62, 63].

1.2.5. Skin permeation models

In order to replace animal models in drug testing for skin application, various models have been developed, such as living skin equivalent models and human reconstructed epidermis[32], which are able to mimic human skin to a large extent. These models are mainly commercial (Episkin™, EpiDerm™ and SkinEthic™) and consist of keratinocyte cultures grown at an air-liquid interface [64], resulting in a stratified, highly differentiated, organotypic tissue model of the human epidermis[65], with various methods for quantification of skin permeability having been developed[64], as well as several studies showing the viability of these models as permeation models[65-67].

1.2.6. Stomach permeation models

Although the intended stomach cellular permeation model has not been established yet, some systems have been developed using the NCI-N87 cell line as a gastric epithelial barrier model for drug permeability assays. The NCI-N87 is a human gastric cancer cell line[68], which possess unique properties, such as the capacity to form a tightly cohesive epithelium, with the expression of adhesion proteins, such as E-cadherin and zonula-occludens-1, a long post-confluency stability and the expression and production of gastric mucin, lipases, pepsinogens and zymogens[69].

Studies with NCI-N87 monolayers obtained moderately high TEER values, as well as mucus production and low apparent permeability coefficients with the passage of integrity markers, such as Lucifer Yellow, thus establishing this cell line as a potential model for gastric drug permeability assays[5]. Other model using a monolayer of NCI-N87 and AGS human epithelial gastric adenocarcinoma cell lines seeded onto Matrigel has been developed, showing the formation of a tightly-knit monolayer, sustainable for the study of the permeability of a simulated gastric epithelium [8].

1.5. Objectives

The main objective of this project was to establish and optimize a triple co-culture (fibroblasts, macrophages and epithelial cells) *in vitro* cellular model of the gastric wall capable of replicating its morphological architecture and function, to be used for permeability, toxicity and functional assays.

One of the first steps to achieve this goal consists in assessing the barrier capabilities of the formed model and its integrity over time. For that purpose, TEER measurements will be carried out over time and permeability assays will be conducted for different cell culture conditions and different combinations of cell densities, with the purpose of determining the

optimal combination yielding a combination of high TEER values with low values of apparent permeability.

Finally, it is imperative to morphologically, structurally and functionally characterize the obtained models. To comply with this objective, different cytochemical and histological analyses will be performed, recurring to inverted fluorescence microscopy (IFM), confocal microscopy and Transmission Electron Microscopy (TEM).

- This page was intentionally left blank. -

Chapter 2

Materials and Methods

2.1. Establishment of an Epithelial Gastric Wall Model

2.1.1. Cell culture

The MKN28 cell line is an immortalized human epithelial gastric adenocarcinoma cell line, first established by Motoyama [70] from a moderately differentiated tubular adenocarcinoma (intestinal-type adenocarcinoma) and was used to simulate the gastric epithelium, since it is easier to maintain and expand in culture, while expressing tight junction markers, such as occludin and claudin[71, 72].

The NST20 cell line (kind gift from Dr. Luis Filipe Silva from IPATIMUP), an immortalized fibroblast cell line isolated from normal human stromal tissue was used to simulate the fibroblasts and the connective tissue present in the gastric mucosa.

The human monocytic leukemia cell line, THP-1, was established by Tsuchiya *et. Al* (1980) [73] and was differentiated into macrophages with PMA (phorbol-12-myristate-13-acetate) [74], in order to simulate the immunitary response found in the stomach wall, similarly to other tissues.

MKN28 (Passage 46-60), NST20 (Passage 14-33) and THP-1 (Passage 27-34) were cultured at 37ºC in humidified atmosphere of 5% CO_2, in RPMI 1640 culture medium (Gibco, UK,) supplemented with 10% v/v heat inactivated Fetal Bovine Serum (FBS) (Gibco, U.K.,) and 1% v/v Penicillin- Streptomycin (P/S) (Westpoint, U.S.A).

Culture medium was changed every two to three days and the cells were routinely sub-cultured, being detached using a 0.25% w/v Trypsin-EDTA solution (Sigma Aldrich, Germany, for 5 min at 37ºC, centrifuged at 1200 RPM for 5 minutes and resuspended in RPMI 1640 culture medium, before seeding in 25 cm^2 and 75 cm^2 flasks, at a cell density of 0.5×10^6 and 1×10^6 cells, respectively (Thermo Scientific, U.S.A) [75, 76].

2.1.2. THP-1 cell line differentiation

Incubation with PMA activates protein kinase C, which induces a high degree of differentiation in THP-1 cells, with an increased adherence and expression of surface markers associated with macrophage differentiation, as well as characteristic morphological changes [74, 77].

THP-1 cells were incubated at a cell density of 5×10^5 cells/ml with PMA (Sigma Aldrich, Germany,) at a concentration of 0.5µL/ml for 48-72h, using the same culture conditions described above [77].

2.1.3. Cell seeding

MKN28, NST20 and THP-1 differentiated cells were cultured in 24-well culture plates (Corning, U.S.A), either on Polyethylene terephthalate BD Falcon™ transwells inserts with no coating (BD, U.S.A) or on BD BioCoat™ Matrigel invasion chambers (BD,U.S.A), both with 8µm size pores.

NST20 cells or NST20 and THP-1 differentiated cells were seeded on the apical side of the insert (500µL of cell suspension were added to the apical chamber, while 750µL of RPMI 1640 culture medium supplemented with 10%v/v heat inactivated FBS and 1% v/v P/S were added to the basolateral chamber) and maintained at 37ºC in an atmosphere of 5% CO_2/95% O_2. After 24 hours, the culture medium was removed from the inserts, and the apical chambers were coated with either BD™ Matrigel™ or BD™PuraMatrix™ (BD, U.S.A), according to the manufacturers' recommendations. After the coating, MKN28 cells were added to the apical chamber of the inserts (500µL of cell suspension were added to the apical chamber, while 750µL of RPMI 1640 culture medium supplemented with 10%v/v heat inactivated FBS and 1% v/v P/S were added to the basolateral chamber) and maintained at 37ºC in an atmosphere of 5% CO_2/95% O_2. A schematic representation of the model created can be found in Fig. 3.

Culture medium was changed every two to three days.

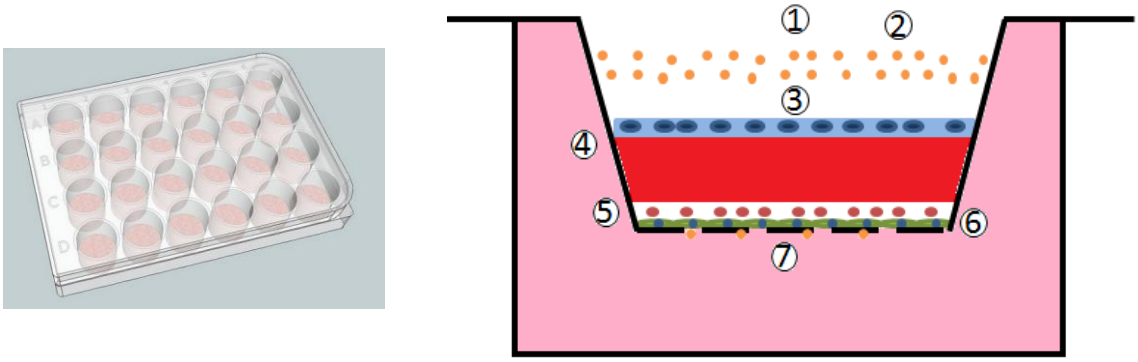

Figure 3- Schematic of the devised *in vitro* gastric mucosa model. 1- Apical Chamber; 2- FITC-dextran; 3- Gastric cell line; 4- BD™Matrigel or BD™PuraMatrix; 5- Macrophages; 6- Fibroblasts; 7- Basolateral chamber.

2.1.4. Matrigel™ or PuraMatrix™ coating

Matrigel™ (BD Biosciences, U.S.A) and PuraMatrix™ (BD Biosciences, U.S.A,) coatings were performed according to the manufacturers' recommendations for 3D matrixes for cell cultures.

Matrigel™ was diluted at a 1:1 rate with RPMI 1640 culture medium, not supplemented with FBS, and after the culture medium was extracted from the inserts, 15 or 30µL of the resulting solution were added to the apical chamber of each insert and maintained at 37ºC in an atmosphere of 5% CO_2/95% O_2 for 1 hour.

PuraMatrix™ was diluted with ${}_dH_2O$ and 20% sucrose (Sigma-Aldrich, Germany), at a dilution rate of 1:1:2, respectively. After the culture medium was removed from the inserts, 30µL were added to the apical chamber and 250µL of RPMI 1640 culture medium supplemented with 10%v/v heat inactivated FBS and 1% v/v P/S were added to the basolateral

chamber of each insert. After 5 minutes, 400µL of RPMI 1640 culture medium supplemented with 10%v/v heat inactivated FBS and 1% v/v P/S were added to the apical chamber and were then maintained at 37ºC in an atmosphere of 5% CO_2/95% O_2 for 1 hour. Approximately 2/3 of the culture medium on the apical chamber were then removed and replaced with fresh medium. This procedure was repeated twice, every half hour.

2.2. Assessment of membrane integrity

Membrane integrity was assessed by measuring the Trans-Epithelial Electrical Resistance (TEER), since a greater resistance is correlated with a greater integrity of the membrane, and the presence of tight junctions, which exist when an epithelial monolayer is correctly formed.

TEER measurements were taken every day or every two days recurring to an Electric-Volt-Ohm Meter device from Millipore® (U.S.A), Millicell ERS-2 Volt-Ohm Meter and an EVOM2, Epithelial Volt-ohm meter, from World Precision Instruments (U.S.A).

Prior to every measurement, the electrodes were bathed in 70% ethanol, for decontamination, washed with Phosphate Buffered Saline (PBS, Sigma Aldrich) and were pre-equilibrated with culture medium for 5 minutes.

Duplicate measurements were performed for each insert and the computed values were obtained by deducting the resistance values of the insert filter alone and the culture medium and multiplying it by the surface area of the transwell (0,33cm^2) [78, 79].

2.3. *In vitro* permeability studies

2.3.1. Permeability Assays

Transwells with different conditions were used after 5, 7 or 8 days in culture, depending on the model tested. Permeability studies were performed using Fluorescein isothiocyanate-dextran (FITC- dextran, Sigma-Aldrich, Germany), a fluorescent marker for paracellular transport, used in cell permeability assays, which can be correlated with the integrity of the membrane.

After cell-washing and equilibration in Hanks Buffer Salt Solution (HBSS, Gibco, U.K.), which was used to ensure a sufficient supply of calcium to cells, in order to maintain cell adhesion and tight junction integrity, 500 µL of FITC-dextran solution at a concentration of 200µg/ml were added to the apical chamber, while 750µL of only HBSS were added to the basolateral chamber.

Eight time-points were performed in total, and every 15 minutes, 100µL were recovered from the basolateral chamber, directly to a black micro-assay 96-well plate (Greiner Bio-one, Austria) and substituted with 100µL of free FITC-dextran HBSS. After 2 hours, 100 µL were also recovered from the apical chamber for analysis by fluorimetry.

The plates were maintained at 37ºC with a continuous agitation of 100 RPM during the course of the experiment.

TEER measurements were also performed every hour during the assay to assess membrane viability [78, 79].

2.3.2. Fluorimetry

The collected samples (100µL) were transferred to a black micro-assay 96-well plate (Greiner bio-one). Calibration curve (Fig. 4) was obtained by using solutions with known concentrations of FITC-dextran (200, 100, 50, 25, 12.5, 6.25, 3.125, 1.56, 0.78 and 0.39µg/ml). Fluorescence was read using a BioTek® Synergy MX (USA) multi-plate reader at an emission/excitation wavelength of 520nm/495nm, respectively.

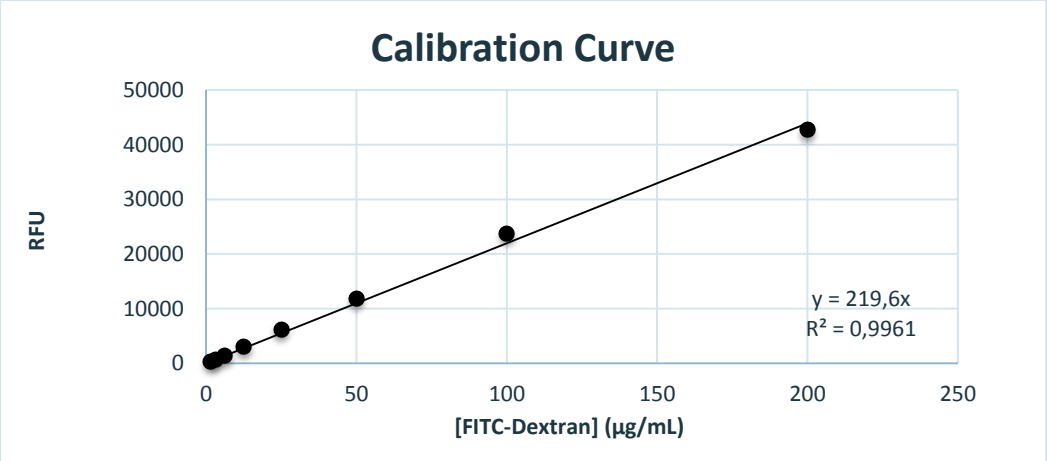

Figure 4- Calibration curve for FITC-dextran for known standard concentrations.

The apparent permeability was calculated taking in consideration the calibration curve (Fig. 4) and by calculating the concentration and mass of FITC-dextran in each sample using equation 1, where $\underline{P_{app}}$ is the apparent permeability in cm/s, **Q** is the concentration of FITC-dextran in the sample, **A** is the surface area of the insert, **C** is the initial concentration of the solution of FITC-dextran and **t** is the time equivalent to the time point chosen:

$$Papp = Q/(A * C * t) \qquad \text{(Equation 1)}$$

The initial concentration of FITC-dextran used was 200µg/ml, the surface area of the transwells used was 0.33 cm^2 and the time point chosen for the calculations was 1 hour after the start of the assay, since the permeation behaviour is linear within this time range [80, 81].

2.4. Morphological and structural characterization

2.4.1. Hematoxylin/Eosin staining

After 5 to 7 days in culture, membranes were washed thrice with PBS for 5 min and fixed in a 1% (v/v) glutaraldehyde (Sigma-Aldrich, Germany) solution in PBS for 15 minutes at room temperature, washed again thrice with PBS for the removal of the fixating agent and fixed in a 4% (v/v) paraformaldehyde solution (PFA, Sigma Aldrich, Germany) in PBS for 1 hour, again at room temperature.

Samples were then dehydrated in an ethanol series (50, 70, 96 and 100% ethanol) for 10 minutes in each solution and were embedded in paraffin for 2 hours. This tissue processing

was performed in a Paraffin tissue processor Microm STP 120-2 and the paraffin embedding in a Modular embedding system Microm EC 350-1/2.

The membranes were cut in 3µm sections for histological analysis using a Leica RM 2255 microtome (Leica, Germany).

Sections were deparaffinised in xylene (AGA, Portugal) (thrice, 8 minutes each time) and hydrated in a descending series of ethanol (100%, 96%, 70% and 50%) for 4 minutes and then in distilled water for 4 minutes. Slides were incubated in Gill's hematoxylin (Sigma-Aldrich, Germany) for 4 minutes and washed in tap water for 3 minutes, after which they were incubated in an ascending series of ethanol (50, 70 and 96% ethanol) for 4 minutes in each solution and stained with Alcoholic Eosin (Leica, U.K.) for 3 minutes, after which they were quickly washed in ethanol 100% and diaphanized in xylene (thrice, 8 minutes each time). Finally they were covered with coverslips using DPX™ mounting solution (Merck, Germany) and visualized using a Zeiss (Germany) Axiovert 200M inverted fluorescence microscope and analysed using AxioVs40 v4.8.2.0 software.

2.4.2. Confocal Microscopy

For Confocal Microscopy, 6-well transwells (Corning, U.S.A) and 24-well coverslips were used instead of the regular 24-well transwells, due to technical problems found when the membrane was cut in sections using microtome (detachment of the cells). A similar procedure for cell culture was used, with cell densities and volumes adapted proportionally to the surface area of the 6-well transwell (4,67cm^2) and the 24-wells (1,91cm^2).

After 5 to 7 days in culture, membranes were washed thrice with PBS for 5 min and fixed in a 1% (v/v) glutaraldehyde solution in PBS for 15 minutes at room temperature, washed again thrice with PBS for the removal of the fixating agent and fixed in a 4% (v/v) paraformaldehyde solution in PBS for 1 hour, again at room temperature.

Cells were then washed thrice in PBS for the removal of the fixating agent and incubated in blocking solution (PBS+ 10% (v/v) FCS) for 6 hours at room temperature. Blocking solution was changed every two hours.

The 6-well transwell was sliced with the aid of a scalpel into four parts, which were moved into 24-well coverslips.

Vimentin staining was obtained by incubating the membranes with primary Vimentin Rabbit mAB antibody from Santa Cruz Biotechnology (U.S.A) at a dilution rate of 1:100 in blocking solution, overnight at 4ºC. The membranes were washed thrice with blocking solution, every 20 minutes and were then incubated with the secondary antibody, Alexa Fluor®594 Rabbit Anti-Mouse from Invitrogen (U.S.A) at a dilution rate of 1:500 in blocking solution for 2 hours.

F-Actin staining was obtained by incubating the membranes with Alexa Fluor® 488 phalloidin probe from Invitrogen (U.S.A) in blocking solution for 1 hour at room temperature.

Finally, the membranes were washed thrice, every 20 minutes, with PBS and were then incubated with 4',6-diamidino-2-phenylindole (DAPI, Sigma Aldrich, Germany), at a dilution rate of 1:10000 (the concentration of the initial stock solution was of 1mg/ml) for nuclei staining for 10 minutes and mounted in Fluoromount™ Aqueous Mounting Medium (Sigma Aldrich, Germany, #F4680-25mL)for 30 minutes.

Confocal microscopy images were obtained using a Laser Scanning Confocal Microscope Leica TCS SP5II confocal microscope (Leica Microsystems, Wetzlar, Germany) and were analysed using FijiImageJ 1.48v software.

2.4.3. Inverted Fluorescence Microscopy

For Inverted Fluorescence Microscopy, 6-well transwells and 24-well coverslips were used instead of the regular 24-well transwells, due to technical problems found when the membrane was cut in sections using microtome (detachment of the cells). A similar procedure for cell culture was used, with cell densities and volumes adapted proportionally to the surface area of the 6-well transwell (4,67cm^2) and the 24-wells (1,91cm^2).

After 5 or 7 days in culture, cells were washed thrice with PBS for 5 min and fixed in a 1% (v/v) glutaraldehyde solution in PBS for 15 minutes at room temperature, washed again thrice with PBS for the removal of the fixating agent and fixed in a 4% (v/v) paraformaldehyde solution in PBS for 1 hour, again at room temperature.

Cells were then washed thrice in PBS for the removal of the fixating agent and incubated in blocking solution (PBS+ 10% (v/v) FCS) for 6 hours at room temperature. Blocking solution was changed every two hours.

The 6-well transwell was sliced with the aid of a scalpel into four parts, which were moved into 24-well coverslips.

Vimentin staining was obtained by incubating the membranes with primary Vimentin Rabbit mAB antibody from Santa Cruz Biotechnology (U.S.A) at a dilution rate of 1:100 in blocking solution, overnight at 4ºC. The membranes were washed thrice with blocking solution, every 20 minutes and were then incubated with the secondary antibody, Alexa Fluor®594 Rabbit Anti-Mouse from Invitrogen (U.S.A) at a dilution rate of 1:500 in blocking solution for 2 hours.

F-Actin staining was obtained by incubating the membranes with Alexa Fluor® 488 phalloidin probe from Invitrogen (U.S.A) in blocking solution for 1 hour at room temperature.

Finally, the membranes were washed thrice, every 20 minutes, with PBS and were then incubated with 4',6-diamidino-2-phenylindole (DAPI) at a dilution rate of 1:10000 (the concentration of the initial stock solution was of 1mg/ml) for nuclei staining for 10 minutes and mounted in Fluoromount™ Aqueous Mounting Medium (Sigma Aldrich, Germany) for 30 minutes.

Inverted Fluorescence Microscopy images were obtained using a Zeiss (Germany) Axiovert 200M inverted fluorescence microscope and analysed using AxioVs40 v4.8.2.0 software.

2.4.4. Transmission Electron Microscopy

After 5 days in culture, membranes were washed thrice with PBS for 5 min and fixed in a 2.5% (v/v) glutaraldehyde (Merck, Germany) solution in Cacodylate buffer (pH 7.2) for 30 minutes at room temperature, washed again thrice for 10 minutes with Cacodylate buffer, for the removal of the fixating agent and fixed in a 1% (v/v) osmium tetroxide solution in Cacodylate buffer overnight at room temperature.

Membranes were again washed thrice for 10 minutes in Cacodylate buffer for the removal of the fixating agent and dehydrated in a series of solutions with an increasing amount of ethanol (25, 50, 70, 96 and 100% ethanol), for 5 minutes in each solution at room temperature.

Membranes were then infiltrated in a solution of Epon and 100% ethanol (1 part Epon/2 parts 100% Ethanol) for 1 hour at room temperature, followed by another hour in a solution of

Epon and 100% ethanol (1 part Epon/1 part 100% Ethanol) and were left to infiltrate overnight in a solution of 2 parts resin/1 part 100% ethanol.

Finally, the membranes were infiltrated in 100% Epon for 1 hour at room temperature and were then left to polymerize for 48 hours at 60ºC.

Transmission Electron Microscopy (TEM) images were obtained using an Electron microscope Zeiss model EM 902 and were treated using FijiImageJ 1.48v software.

2.5. Statistical analyses

Statistical analysis was performed using GraphPad Prism 5 software. Mean and standard deviation were calculated for each sample.

Independent samples were considered significantly different if a difference of $P < 0.05$ was obtained in the independent samples two-tailed Student's t-test for samples that followed a normal distribution.

- This page was intentionally left blank. -

Chapter 3

Results and Discussion

The main goal of this work was to establish a cellularized artificial model of the gastric wall. In order to do so, several combinations of cell densities and coatings were tested, with the purpose of finding the optimal cell combination, which best replicates the gastric epithelium, as well as the subjacent extracellular matrix (ECM) and connective tissue, while also enabling an immune response.

Several tests were performed in different models to assess membrane integrity, as well as the apparent permeability of these models to a fluorescent paracellular marker (FITC-dextran), which is an important factor if they are to be used in drug testing.

Morphological and structural characterization was also performed, with the purpose of assessing the constitution of the proposed models.

3.1. Membrane integrity assessment

Membrane integrity was assessed through TEER measurements, since a high TEER value is correlated with the presence of tight junctions, which exist when a tightly-knit epithelium layer is formed [79, 82], and are responsible for the control of solute movement though a paracellular pathway [83]. Thus, TEER values can be correlated with membrane integrity, since a correctly formed epithelial layer will possess more tight junctions, which in turn will constitute an obstacle to the passage of ions, resulting in high TEER values. However, the measurement of the TEER is not an absolute indicator of membrane integrity [84], and as such these results should rather be taken as a relative indicator of membrane integrity, which should be complemented with other tests.

3.1.1. Influence of Matrigel

Throughout the establishment of the gastric mucosa models, two different volumes (15 and 30µL) of BD™ Matrigel™ were used to perform a coating over the fibroblasts, simulating the extracellular matrix found *in vivo*. Matrigel is a complex protein gelatinous mixture secreted by Engelbreth-Holm-Swarm (EHS) mouse sarcoma cells, which resembles the complex extracellular environment found in many cells and is therefore used as a substrate for cell culture [85]. However, this leads to great variability in its contents, thus making it highly irreproducible.

3.1.1.1. Influence of Matrigel™ coating volume

Initially three different volumes of Matrigel™ were used (15, 30 and 60µL) and compared to BD BioCoat™ Matrigel invasion chambers, considering their influence on the homogenous formation of the membrane, and its respective integrity. BD BioCoat™ Matrigel invasion chambers are commercially available transwells that are previously coated with Matrigel. Although the exact volume used to perform this coating is unknown, it is done through an industrial process and therefore it allows for a more homogenous coating, to which it is possible to compare the influence of the Matrigel coating on the barrier integrity. These results can be observed in Fig. 5.

The first assays were performed using a 15µL Matrigel™ coating to simulate the *lamina propria*, in addition to the fibroblasts and epithelial cells used for the formation of the barrier model. However, it was observed that correct barrier formation did not always occur, showing low reproducibility. It is supposed this was due to the fact that this amount of BD™ Matrigel™ was insufficient to provide a homogenous coating, leading to the formation of air bubbles, hence inhibiting cellular growth and the ordered establishment of an epithelial barrier. These effects were translated into high standard deviations, impairing the correct comparison between the different experimental conditions, as can be seen by observing Figs. 5-8 A.

Considering the above mentioned difficulties, it was hypothesized that a greater volume of Matrigel™ could improve the experimental results, by providing a more homogenous coating and barrier formation, while not influencing the TEER values obtained. In Fig. 5 it is possible to observe that no significant differences were observed between the three volumes tested when the barriers were correctly formed. Bearing this in mind, the volume of 30µL was chosen for further experiments, since it provided enough reliability at a lower cost.

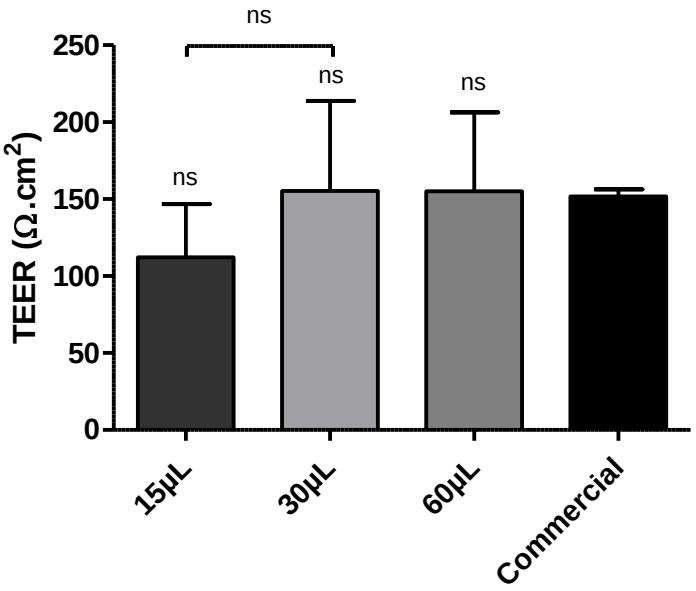

Figure 5 - Influence of Matrigel™ volume coating on TEER, in a "sandwich" model, after 5 days in culture, in comparison to BD BioCoat™ Matrigel invasion chambers (n=2). Samples with ns were considered to be statistically non-significant (P>0.05) when compared to the control group (Commercial) and between them.

3.1.1.2. Influence of model configuration

Different model configurations were tested in order to assess the effect of the relative positioning of the extracellular matrix (represented by the Matrigel™ coating in Fig. 6) within the proposed model on membrane integrity. Therefore, Matrigel™ was used as coating directly in contact with the insert, and also with the cells cultivated on top of the coating. Other configurations used consisted in using the matrigel between the fibroblasts and the epithelial layer, henceforth called "sandwich" model, and finally with the fibroblasts embedded in the Matrigel™ coating. A schematic representation of the different conformations is represented in Fig. 6.

The results, in terms of the TEER values of the different conformations, can be observed in Fig. 7.

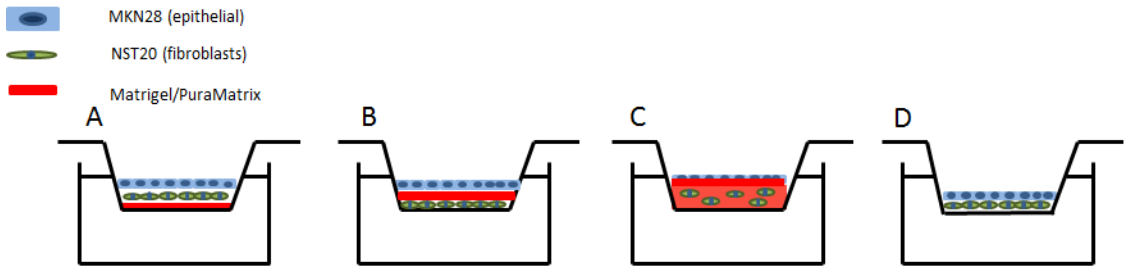

Figure 6 - **Schematic representation of the different configuration models: A- Model with Matrigel/PuraMatrix directly on top of the insert (Direct coating); B- "Sandwich" model; C- Model with fibroblasts embedded in Matrigel/PuraMatrix ; D- Model without Matrigel/PuraMatrix coating (No coating).**

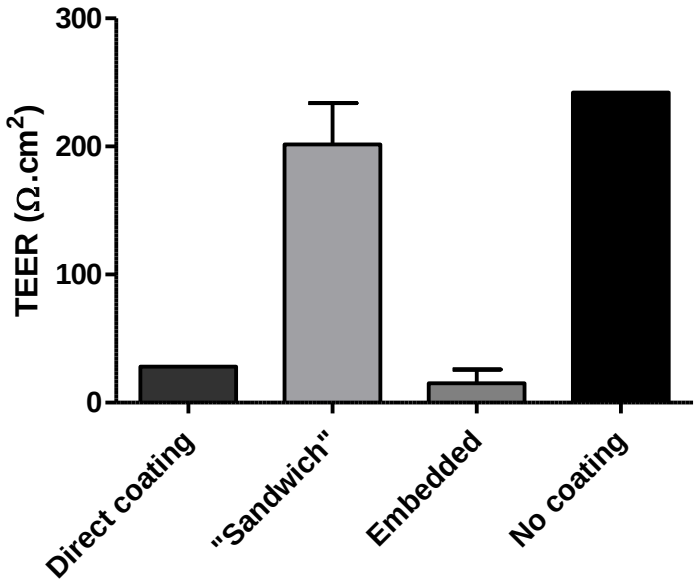

Figure 7 - **Influence of Matrigel™ coating conformation on TEER, after 8 days in culture, when comparing to a condition without coating (n=2).**

Comparing the different conformations, in terms of the integrity of the model, given by the TEER values, it is possible to observe that the model with the direct Matrigel coating and the model with the fibroblasts embedded in the Matrigel do not elicit the formation of an epithelial barrier, since they present low TEER values. On the other hand, the "sandwich" model presented moderately high TEER values, which can be the result of the formation of a cohesive epithelial barrier. Hence, the sandwich model was selected as the standard for future tests, which will be represented from now on in all figures as "model". The reason

behind these results is still unclear, requiring more experiments to fully understand this promising behaviour. However, it is possible to hypothesize that regarding the model without the Matrigel™ coating, the barrier formation is inhibited due to the lack of extracellular matrix components, which provide essential mechanical and biochemical stimuli to the cells. The lower values obtained for the model with the fibroblasts embedded in the Matrigel™ can be explained by the interference of the extracellular matrix with the passage of signalling factors secreted by the fibroblasts, while in the "sandwich" model the epithelial cells can receive the necessary stimuli from the extracellular matrix represented by the Matrigel™, as well as the input supplied by the fibroblasts' secreted extracellular matrix.

3.1.1.3. Influence of fibroblasts' cell density

To understand the influence of the cell density of NST20 fibroblasts in the integrity of the models, four different cell densities were tested (1×10^3; 5×10^3; 1×10^4 and 5×10^4 cells/transwell), while maintaining constant the variable cell density of MKN28 (5×10^4 cells/transwell). Two control conditions (MKN28 5×10^4 and MKN28 5×10^4 cells/transwell coated with Matrigel, without fibroblasts) were also included for comparison, as well as a condition with only NST20 cells and another with NST20 cells with a Matrigel coating.

The results presenting the TEER values over time are shown in Fig. 8, for (A) 15 and (B) 30µL of BD™ Matrigel™ used. Comparisons between the different conditions, after 5 days in culture, are shown in Fig. 9, for 15 and 30µL of Matrigel used.

When a volume of 15µL was used no significant trend or differences could be noticed when comparing the different cell densities. However, when a volume of 30µL was used a trend became apparent, namely a decrease in TEER values as the cell density of NST20 increased. This behaviour can probably be explained by a competition phenomenon, in which the fibroblasts can invade the extracellular matrix and compete with the epithelial cells for nutrients, oxygen and growth space, thus inhibiting the formation of a homogeneous epithelial layer, hence the observed lower TEER values.

Considering all of this, the cell density of 5×10^3 NST20 cells/transwell was selected for further tests, since it enabled high TEER values, while also being high enough to assure that fibroblasts and their physiological contribution can be well represented within the proposed models.

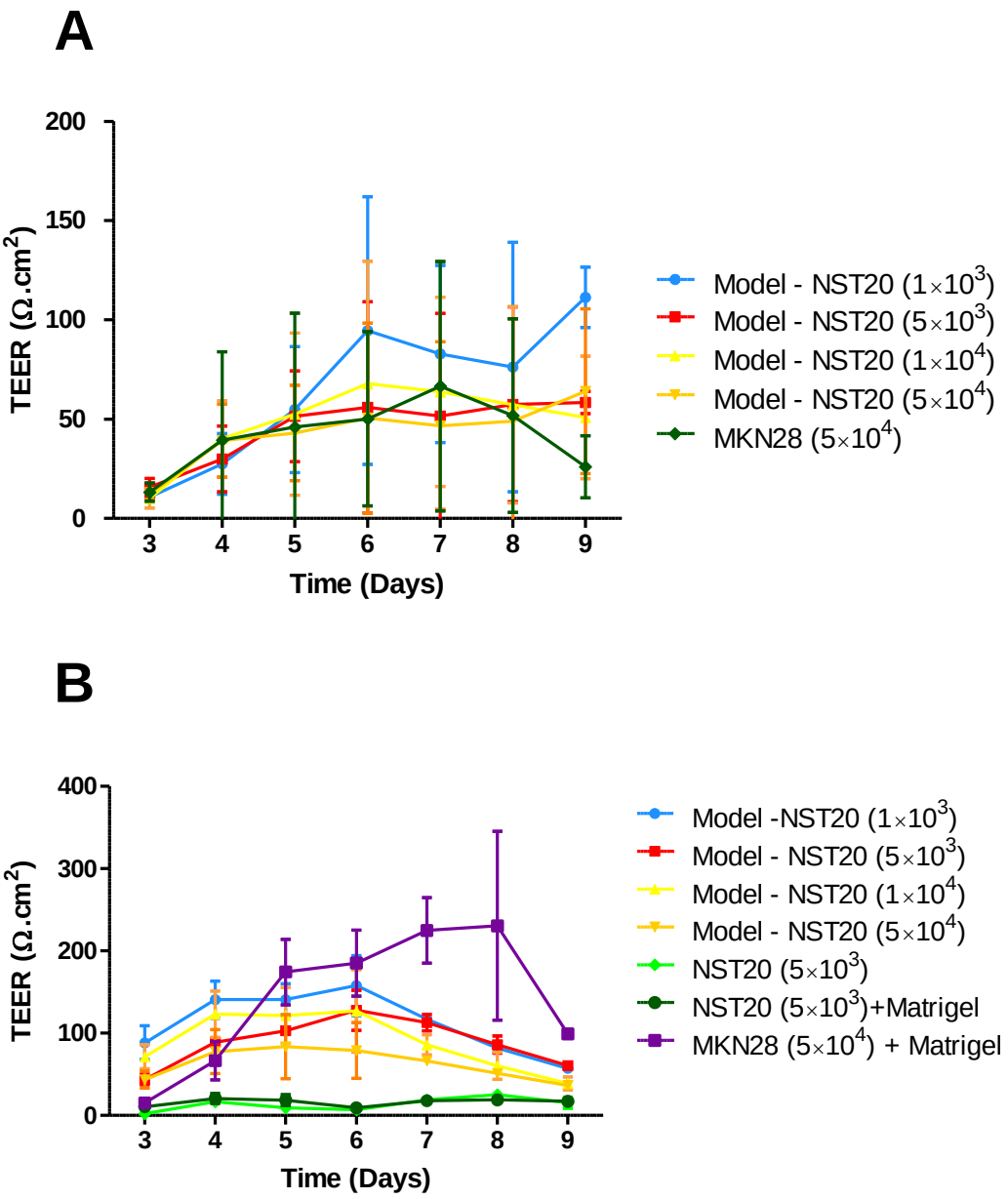

Figure 8- A: Influence of NST20 cell density on TEER, over time, in a "sandwich" model, for a volume of 15µL of Matrigel (n=4); B: Influence of NST20 cell density on TEER, in a "sandwich" model, for a volume of 30µL of BD™ Matrigel (n=3). Note the decrease of the standard deviation values, after the volume of BD™ Matrigel was optimized for 30µl.

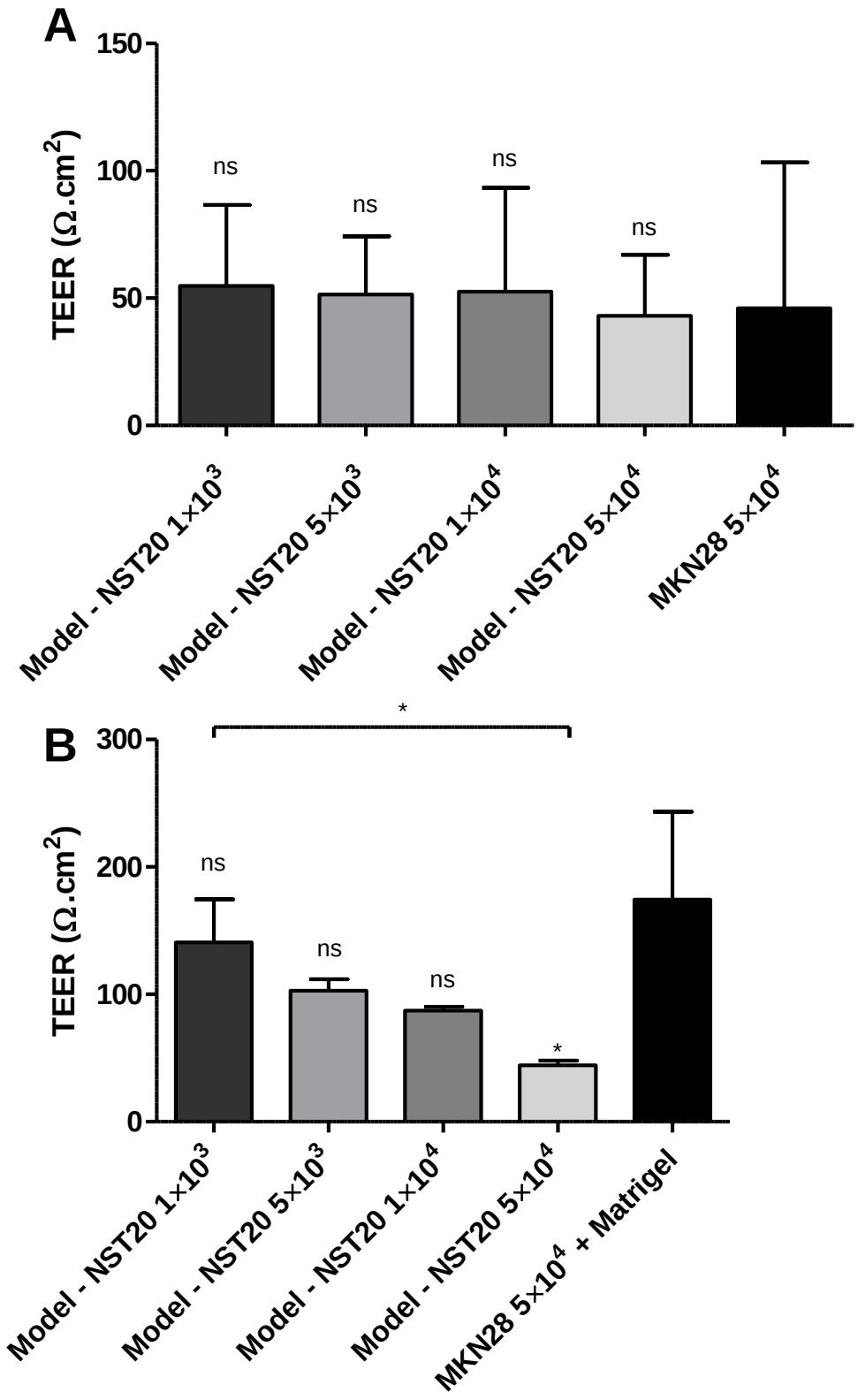

Figure 9- **A: Influence of NST20 cell density on TEER, after 5 days in culture, in a "sandwich" model, for a volume of 15µL of Matrigel (n=4); B: Influence of NST20 cell density on TEER, after 5 days in culture, in a "sandwich" model, for a volume of 30µL of Matrigel (n=3). Samples with ns were considered to be statistically non-significant (P>0.05) when compared to the control group (MKN28 5×10^4+ Matrigel), while samples with * were considered to be statistically significant (P<0.05). Note the decrease of the standard deviation values, after the volume of Matrigel was optimized for 30µl.**

3.1.1.4. Influence of epithelial gastric cells' density

In order to understand the influence of the cell density of MKN28 cells in the integrity of the models, five different cell densities were tested (5×10^3; 1×10^4; 5×10^4; 1×10^5 and 5×10^5 cells/transwell), while maintaining the cell density of NST20 constant (5×10^3 cells/transwell). A control condition (NST20 5×10^3 cells/transwell coated with Matrigel) was also included for comparison, as well as a condition with only MKN28 cells (without coating) and another with MKN28 cells with a Matrigel coating.

The results presenting the TEER values over time are shown in Fig. 10, for (A) 15 µL and (B) 30µL of Matrigel™ used. Comparisons between the different conditions, after 5 days in culture, are shown in Fig. 11, for 15µL and 30µL of Matrigel used.

Results shows that higher TEER values were obtained using higher cell densities of MKN28 cells, while being statistically different when compared to the control group (NST20 cells coated with Matrigel). This suggests that a minimal cell density is necessary for establishing a homogenous epithelial barrier, although no significant differences were found between the highest 3 densities tested (1×10^4 and 5×10^5 cells/transwell). A saturation phenomenon was also achieved after 5-6 days in culture for these cell densities, after which the cells reached a *plateau* and eventually started to deteriorate, possibly due to Matrigel degradation, leading to a decrease in the TEER values. It is also important to notice that the TEER values are lower for the proposed models than those obtained when only using epithelial cells. This can be explained by the fact that the introduction of a 3D matrix might constitute an obstacle to cellular proliferation and cell-cell contact, which are essential to the formation of an homogeneous and a compact epithelium, thus leading to a more disperse architecture, and a more permeable barrier, as well as less cellular proliferation[86]. These values are also found to be within the same range as those found in the literature for a MKN28 monolayer [71].

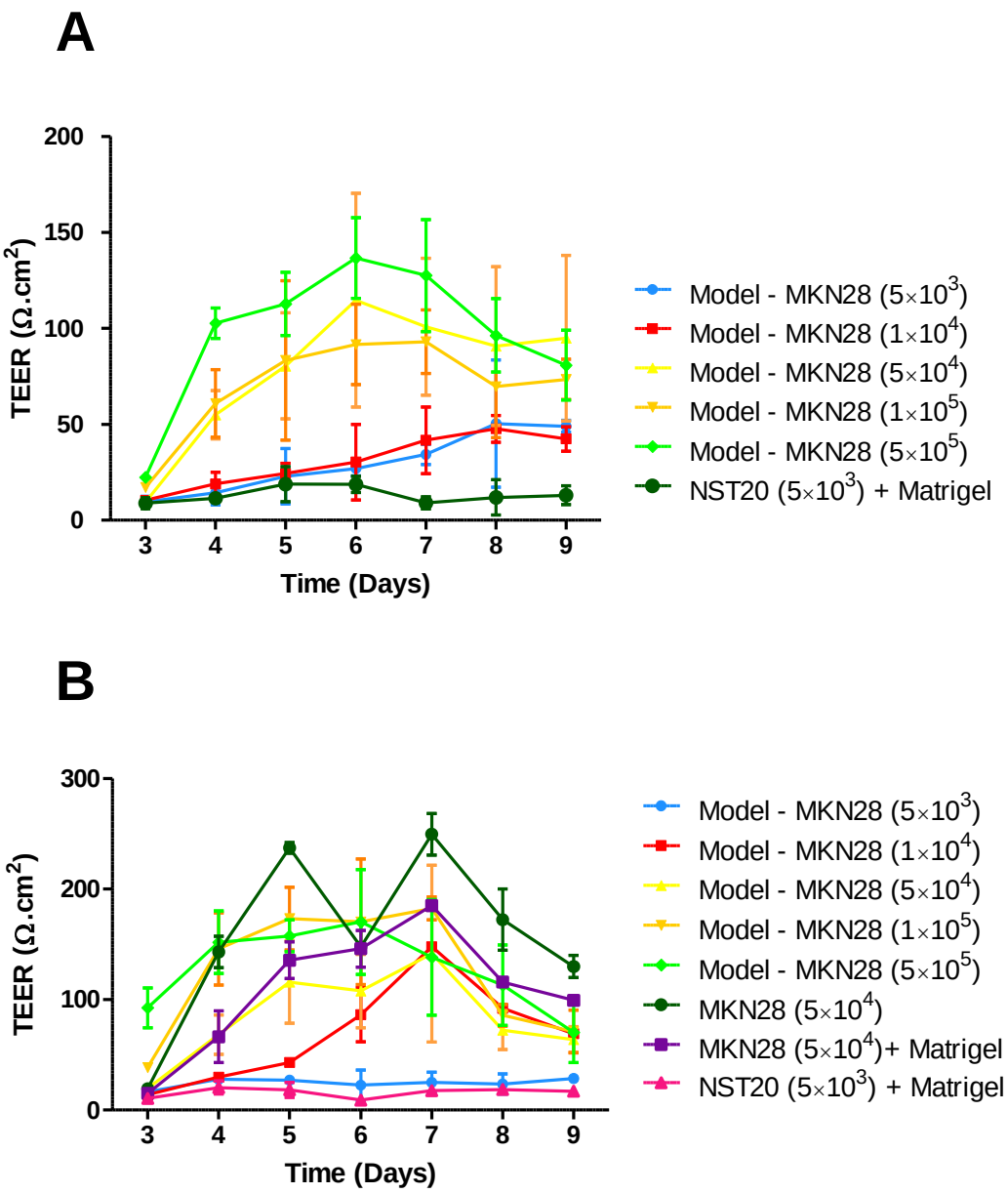

Figure 10 - A: Influence of MKN28 cell density on TEER, over time, in a "sandwich" model, for a volume of 15µL of Matrigel (n=4); B: Influence of MKN28 cell density on TEER, in a "sandwich" model, for a volume of 30µL of BD™ Matrigel (n=3). Note the decrease of the standard deviation values, after the volume of BD™ Matrigel was optimized for 30µl.

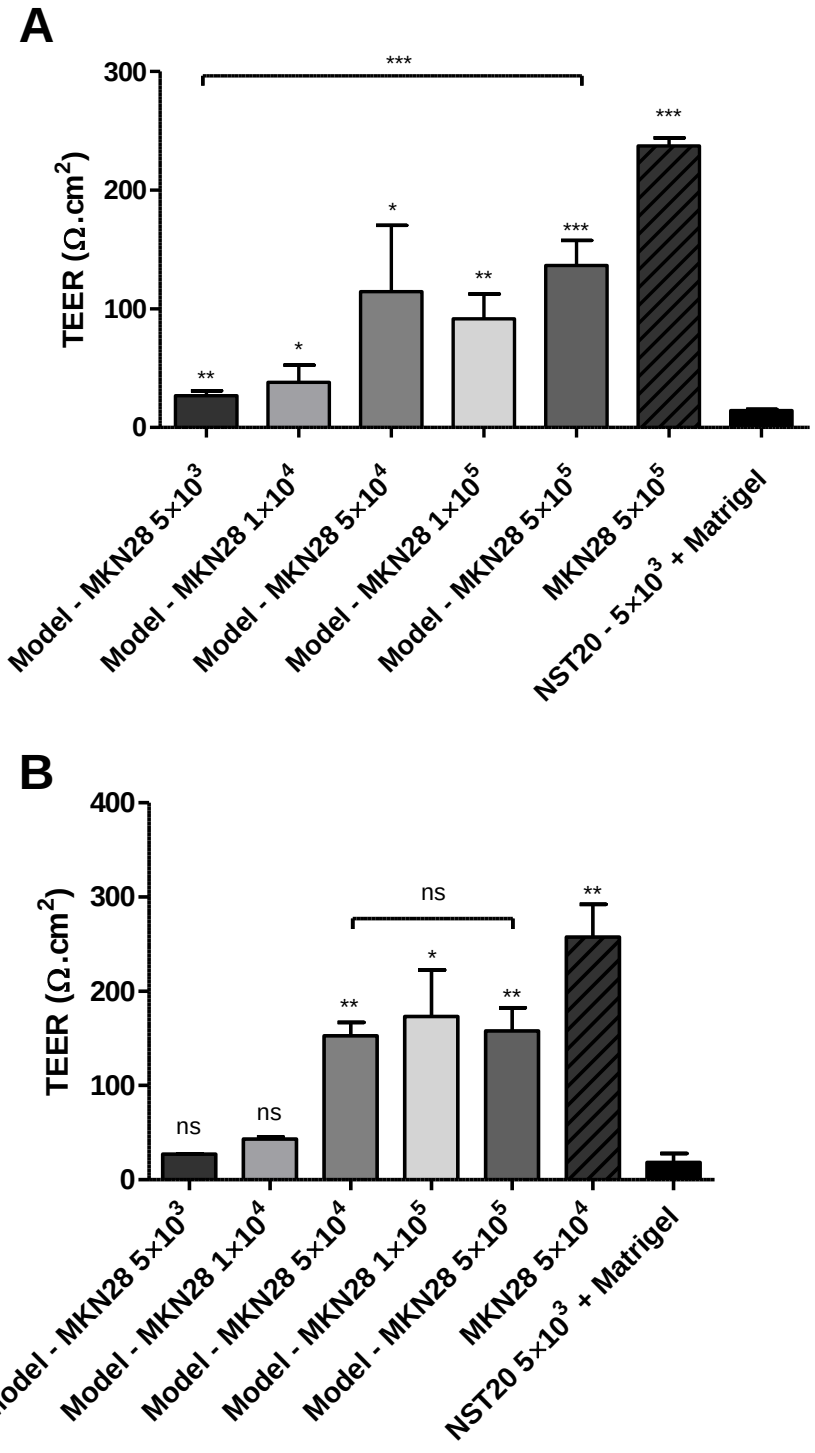

Figure 11 - A: Influence of MKN28 cell density on TEER, after 5 days in culture, in a "sandwich" model, for a volume of 15µL of BD™ Matrigel (n=4); B: Influence of MKN28 cell density on TEER, after 5 days in culture, in a "sandwich" model, for a volume of 30µL of Matrigel (n=3). Samples with ns were considered to be statistically non-significant (P>0.05) when compared to the control group (NST20 5×10³ coated with Matrigel), while samples with * were considered to be statistically significant (P<0.05) and with ** were considered to be highly significant (P<0.01). Note the decrease of the standard deviation values, after the volume of BD™ Matrigel was optimized for 30µl.

3.1.2. Influence of puramatrix

In order to circumvent the disparities in results obtained with the models using matrigel, possibly due to its unpredictable constitution, as previously discussed, alternative models were tested, using puramatrix since it also emulates the extracellular matrix but additionally benefits from being purely synthetic, and thus less variable in nature[87].

Similarly as before, different model conformations were tested in order to assess the effect of the architecture of the extracellular matrix and its relative positioning within the proposed model on the membrane integrity. A schematic representation of the different configurations is represented in Fig. 6. These results obtained can be observed in Fig.12. The model in which a puramatrix coating was performed directly on the insert failed to promote the correct formation of the epithelial barrier, suggesting that a direct contact between puramatrix and fibroblasts might be inhibitory or that the coating needs the support of the extracellular matrix secreted by the fibroblasts in order to achieve the desired outcome. On the contrary, both the "sandwich" model and the one in which the fibroblasts were embedded provided successful outcomes, although resulting in no significant differences between them and the model without any puramatrix. When comparing the embedded results with the results previously obtained with Matrigel, it is observable that when PuraMatrix was used, greater TEER values were obtained. This can possibly be explained by differences in the mesh created by those two ECM substitutes, with PuraMatrix being more permissive and enabling the formation of a tighter epithelium.

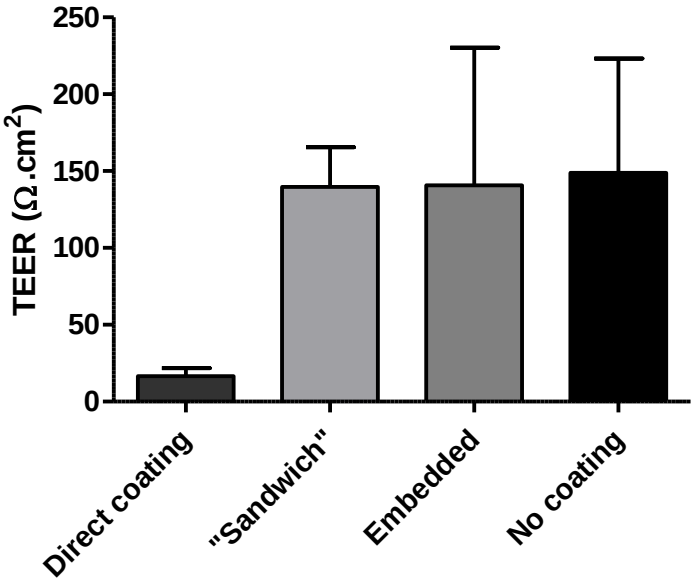

Figure 12 - Influence of Puramatrix™ coating conformation on TEER, after 7 days in culture, when comparing to a condition without coating (n=2).

3.1.2.1. Influence of cell density of macrophages

In order to simulate the immune cells present in the gastric mucosa and to better replicate the *in vivo* conditions, THP-1 derived macrophages, which express characteristic morphological and functional features of normal macrophages, as well as specific macrophage markers [77], were used.

To understand the influence of the cell density of THP-1-derived macrophages in the integrity of the previous co-culture models, three different cell densities were tested (1×10^3, 5×10^3 and 5×10^4 cells/transwell) in PuraMatrix™ coated transwells, while maintaining

the cell density of NST20 and MKN28 constant (5×10^3 and 5×10^4 cells/transwell, respectively). A control condition (without macrophages) was also included for comparison.

The results presenting the TEER values over time, as well the comparisons between the different conditions, after 7 days in culture, are shown in Figs. 13 and 14, respectively.

Results shows that no significant differences were found between the different macrophage densities, when compared to the control condition (Model – No Macrophages) regarding the TEER. This indicates that macrophages probably do not interfere with the TEER, since it is dependent on ion passage, which is not influenced by the presence of macrophages. This is corroborated by the low values obtained for the condition with only macrophages, indicative of the absence of barrier formation.

Considering these results, the cell density of macrophages chosen for further tests was of 5×10^3 cells/transwell, considering that no significant differences were found between the other densities, while being sufficient to be representative of the macrophage influence in the barrier model.

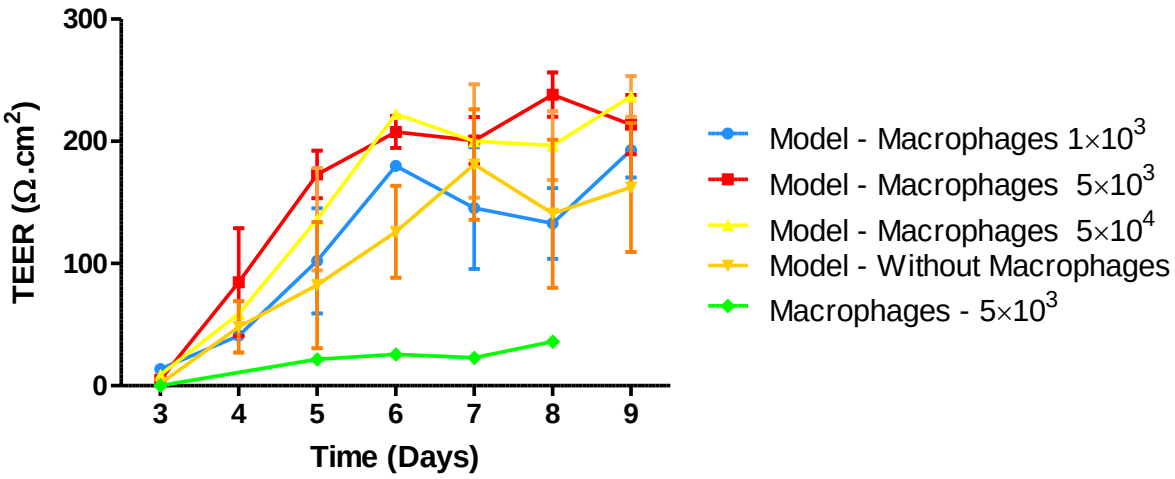

Figure 13 - Influence of the cell density of THP-1-derived macrophages cultured on PuraMatrix coated transwells on TEER, in a "sandwich" model, over time (n=4).

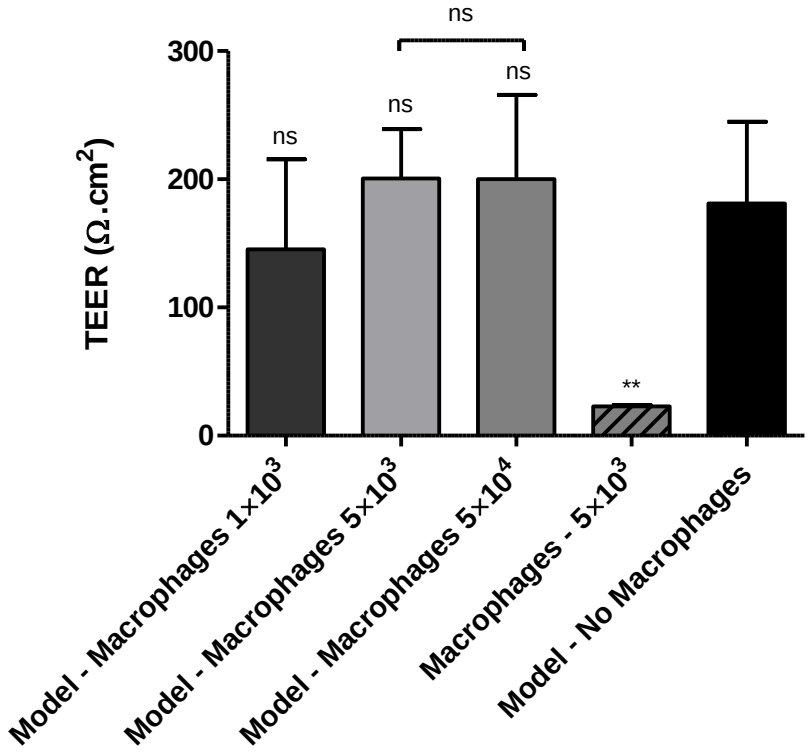

Figure 14 - Influence of the cell density of THP-1-derived macrophages cultured on PuraMatrix™ coated transwells on TEER, after 7 days in culture, in a "sandwich" model, while maintaining the concentration of fibroblasts and epithelial cells constant (5×10^3 and 5×10^4 cells/transwell, respectively) (n=4). Samples with ns were considered to be statistically non-significant (P>0.05) when compared to the control group (Model – No Macrophages) and between them.

3.2. *In vitro* permeability assays

The correct formation of the proposed barrier model is dependent on the existence of a tightly knit cell layer, responsible for the low permeability of this barrier, similarly to what happens *in vivo* [79].

Tight junctions, which are the most apical structures of the epithelial junctional complex, formed by proteins such as claudins and occludins, are responsible for the mediation of paracellular transport across the membrane. This correlates with a greater barrier effect and selective permeability of the membrane to certain solutes (based on particle size or charge), such as calcium and sodium ions or small proteins [83].

In vitro permeability assays with FITC-dextran, a fluorescent marker for paracellular transport, were conducted in order to assess the permeability of the models in study.

3.2.1. Matrigel™ permeability assays

Permeability assays were conducted with models coated with Matrigel™ and the calculated apparent permeability (cm/s) was compared to different control conditions for each of the test conditions optimized before, namely: 5×10^3 NST20 cells/transwell; 5×10^4 MKN28 cells/transwell; 5×10^3 NST20 cells/transwell with a Matrigel coating on top of the fibroblasts 5×10^4 MKN28 cells/transwell in Matrigel coated transwells; transwells with only a Matrigel coating and transwells without cells or coating. An evolution of the quantity of FITC-dextran permeated over time of the different samples can be observed in Fig. 15.

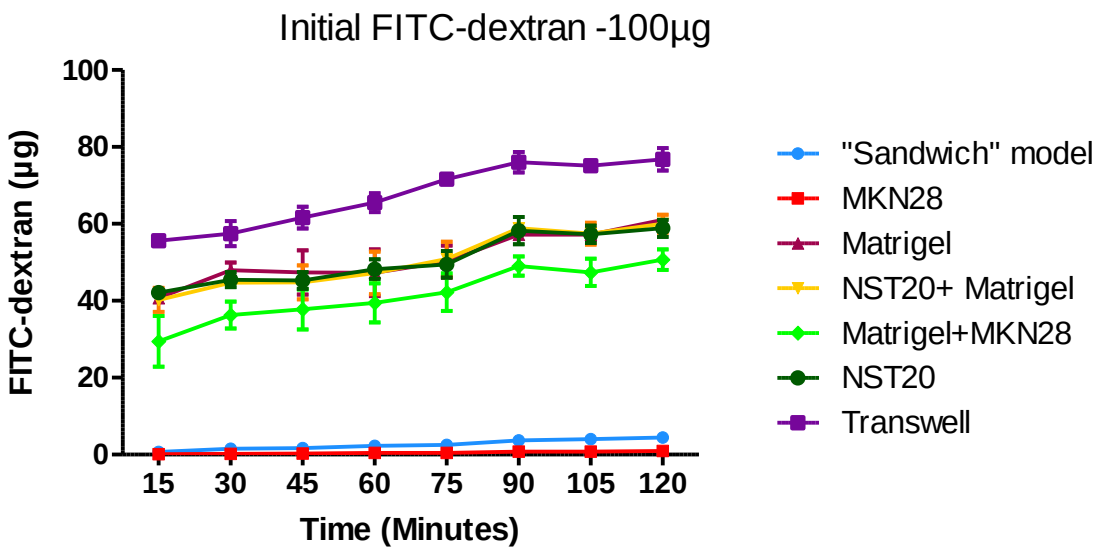

Figure 15 - **Evolution of the quantity of FITC-dextran permeated over time in Matrigel™ coated transwells for the different conditions (n=4).**

A comparison of the apparent permeability of the different samples after 1 h of incubation with FITC-dextran and a comparison between only the proposed models and two control conditions (5×10^4 MKN28 cells/transwell and 5×10^4 MKN28 cells/transwell inMatrigel coated transwells) is represented in Fig. 16, in order to better visualize the differences observed.

The first tests, performed on transwells coated with Matrigel™ with the "sandwich" configuration showed that the barriers without macrophages presented lower values of apparent permeability than the other controls, only being higher than the values obtained for the models formed by only epithelial cells. From among the control conditions, only the one with MKN28 cells presented low values of permeability, since it is the only that could form a cohesive epithelial layer. Other conditions constitute some obstacle to the passage of FITC-dextran (presenting lower apparent permeability values than the condition with only the transwells), but are incapable of forming a restrictive barrier. It is interesting to notice that the control with epithelial cells seeded over Matrigel-coated transwells, once again, showed differences from the control with only epithelial cells, which confirms the TEER values presented before in Fig. 8. This time, the model coated with Matrigel presented higher permeability values, which may be explained by the 3D environment it imposes upon the epithelial cells, hindering their capacity to form a tight epithelial monolayer, which may enable the passage of solutes like FITC-dextran.

The values for the barrier models are in the same range as the ones reported for models in other tissues, such as the intestinal [78], which confirms that these models are within physiological operating capabilities regarding their permeability.

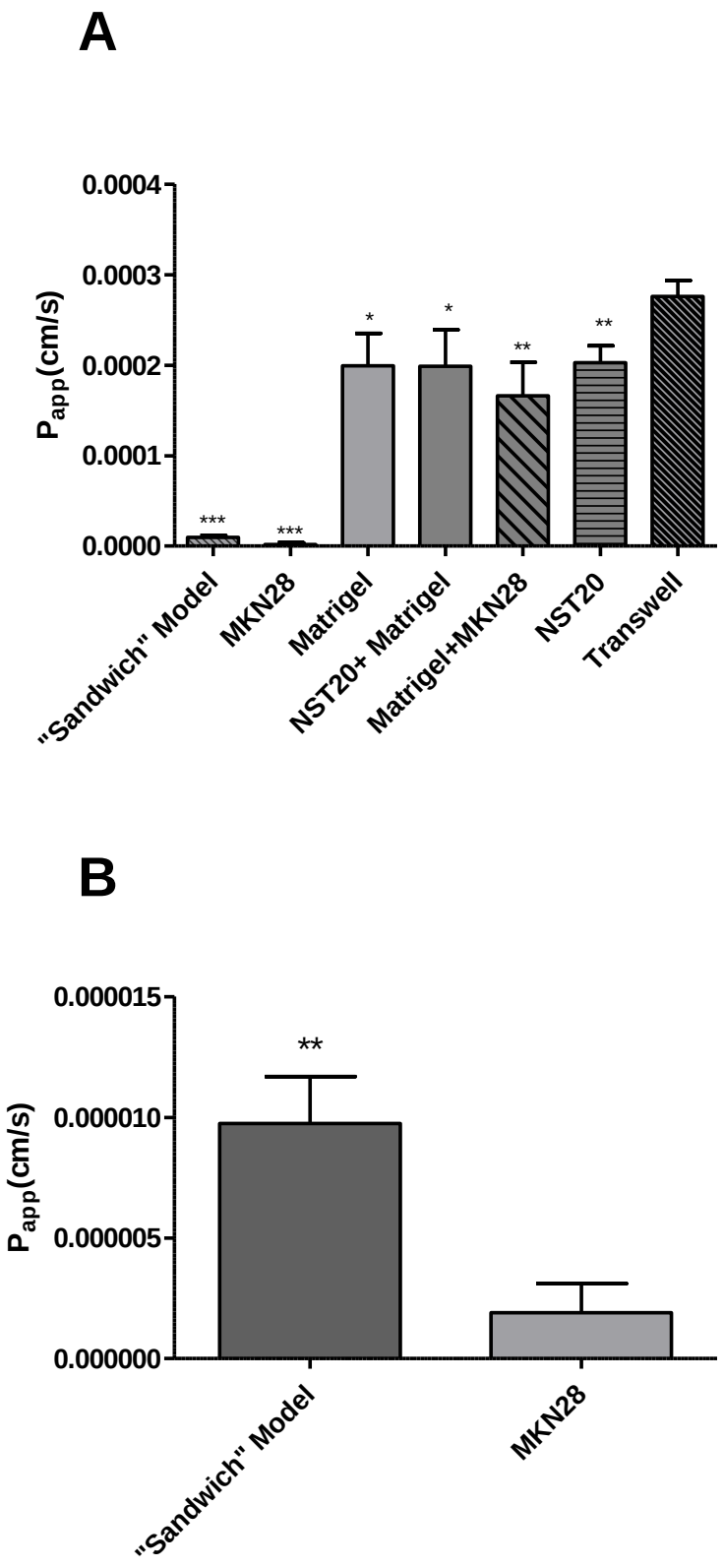

Figure 16 - A: Comparison of the apparent permeability of the different models in Matrigel™ coated transwells with the control condition (Transwell) (n=3). B: Detailed comparison of the apparent permeability of the models in Matrigel™ coated transwells with the control condition (MKN) and with Matrigel+MKN (n=3). Samples with ns were considered to be statistically non-significant (P>0.05) and with * were considered to be statistically significant (P<0.05), while samples with ** were considered highly significant (P<0.01) and with *** extremely significant (P<0.001) when compared to the control group (Transwell and MKN, respectively) and between them.

3.2.2. PuraMatrix™ permeability assays

Considering the already mentioned disparities obtained with the models using Matrigel™, possibly due to its unpredictable nature, models with PuraMatrix™ were tested, in order to assess their permeability. As previously, these models further include macrophages to better emulate the extracellular matrix.

Permeability assays were conducted with models coated with PuraMatrix™ with and without macrophages, in order to assess their influence on the apparent permeability (cm/s), which was compared to different control conditions for each sample, namely: 5×10^3 NST20 cells/transwell, 5×10^4 MKN28 cells/transwell, transwells with only PuraMatrix and transwells without cells or any coating. An evolution of FITC-dextran permeation over time for the different samples can be observed in Fig. 17.

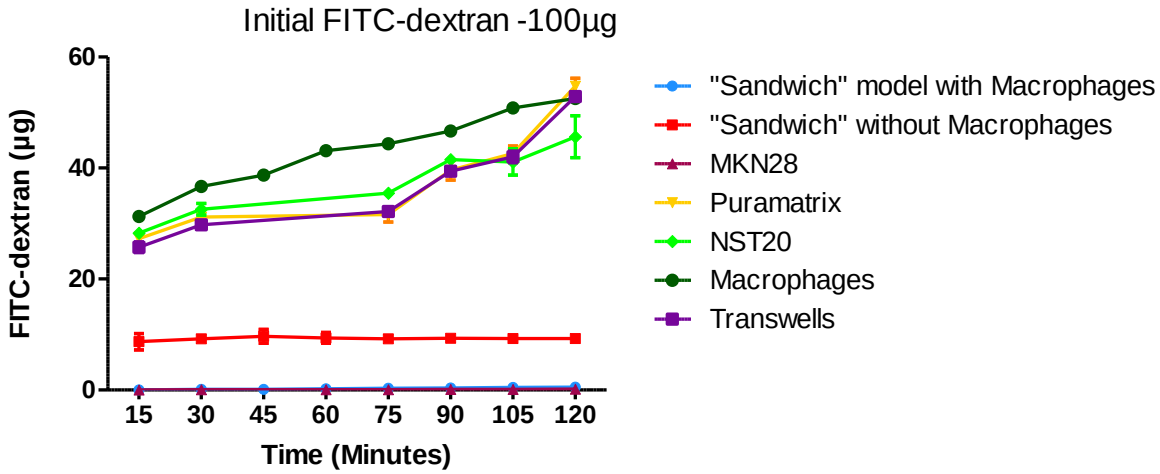

Figure 17 - Evolution of the quantity of FITC-dextran permeated over time in PuraMatrix™ coated transwells for the different conditions (n=4).

A comparison of the apparent permeability of the different samples after 1 h of incubation with FITC-dextran and a comparison between only the proposed models and a control condition (5×10^4 MKN28 cells/transwell) are represented in figure 18, in order to better visualize the differences observed between them.

With the inclusion of macrophages a significant decrease in the apparent permeability was observed, with values even lower than the ones obtained for models where only epithelial cells were used. These results clearly show that macrophages have a decisive impact in the permeability of these barriers, indicating their involvement in the opsonisation and phagocytosis of external particles and/or small molecules such as FITC-Dextran [88], although high permeability values were obtained when only macrophages were used, which is indicative that they alone are not capable of establishing a cohesive cell layer, despite their obvious influence on the apparent permeability.

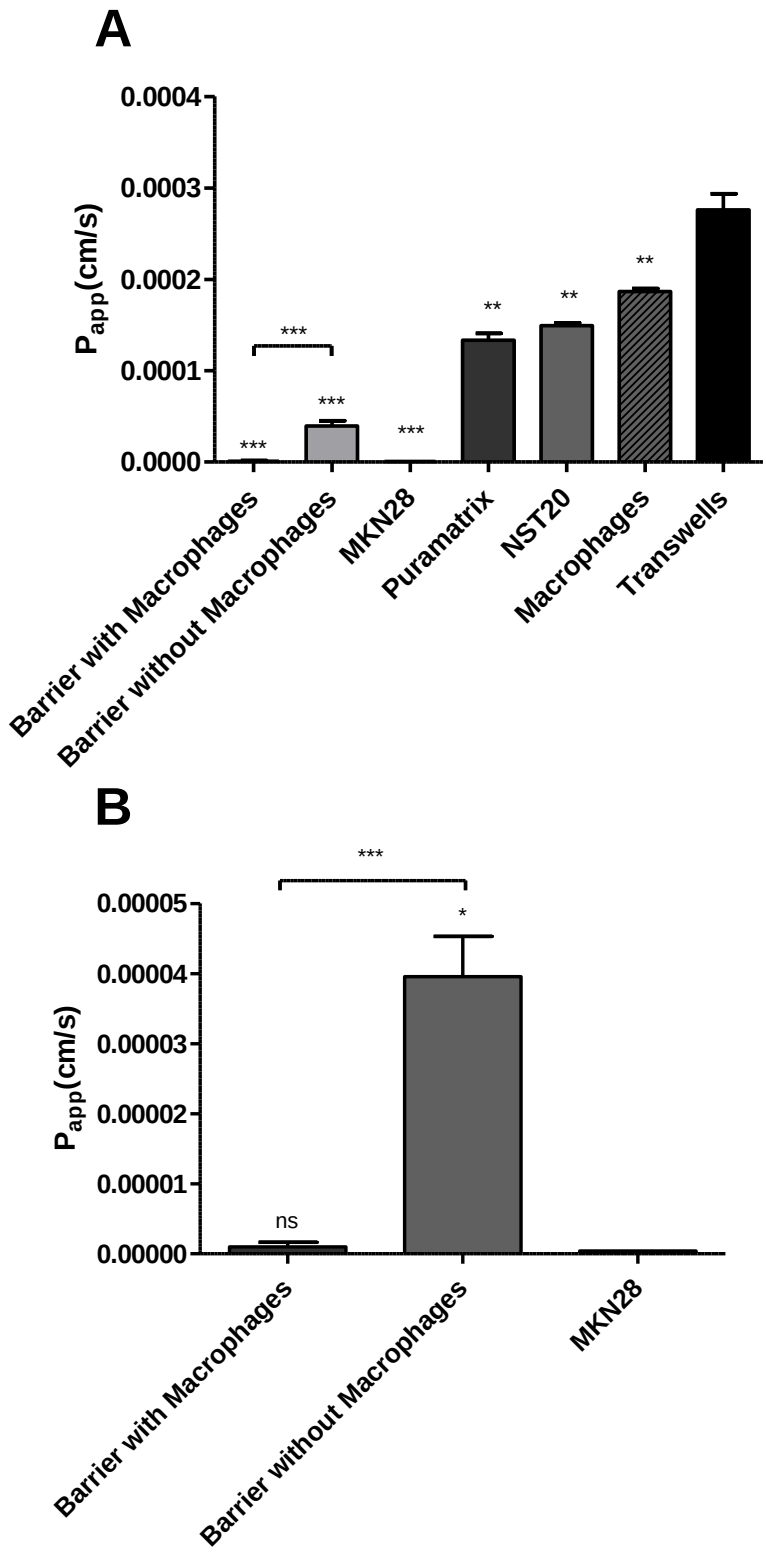

Figure 18 - **A: Comparison of the apparent permeability of the different models in PuraMatrix™ coated transwells with the control condition (Transwell) (n=4). B: Detailed comparison of the apparent permeability of the models in PuraMatrix™ coated transwells with the control condition (MKN) (n=4).**
Samples with ns were considered to be statistically non-significant (P>0.05) and with * were considered to be statistically significant (P<0.05), while samples with ** were considered highly significant (P<0.01) and with * extremely significant (P<0.001) when compared to the control group (Transwell and MKN, respectively) and between them).**

3.3. Morphological and structural characterization

In order to morphologically and structurally characterize the models developed, immunohistochemistry was performed, by staining cells for F-actin which is present in the cytoskeleton of fibroblasts, epithelial cells, and macrophages, for vimentin, which is a specific marker for fibroblasts, and finally for DAPI , which stains the nuclei of all cell types.

A "sandwich" model with PuraMatrix and macrophages was characterized and the images obtained for the different fluorescence channels and the merged results can be observed in Figs. 19 and 20. Through inverted fluorescence microscopy (IFM) it was possible to confirm the formation of a tightly-knit epithelium (using actin staining, in green, and nuclei staining, with DAPI, in blue) on the proposed barrier models, as well as the presence of cells that resemble fibroblasts (with positive staining in red for vimentin, a mesenchymal marker [89], which can also be present in macrophages, although in this case the cell morphology allows to determine it is probably a fibroblast), in an inferior cell layer, thus emulating the *in vivo* anatomical structure and organization [90].

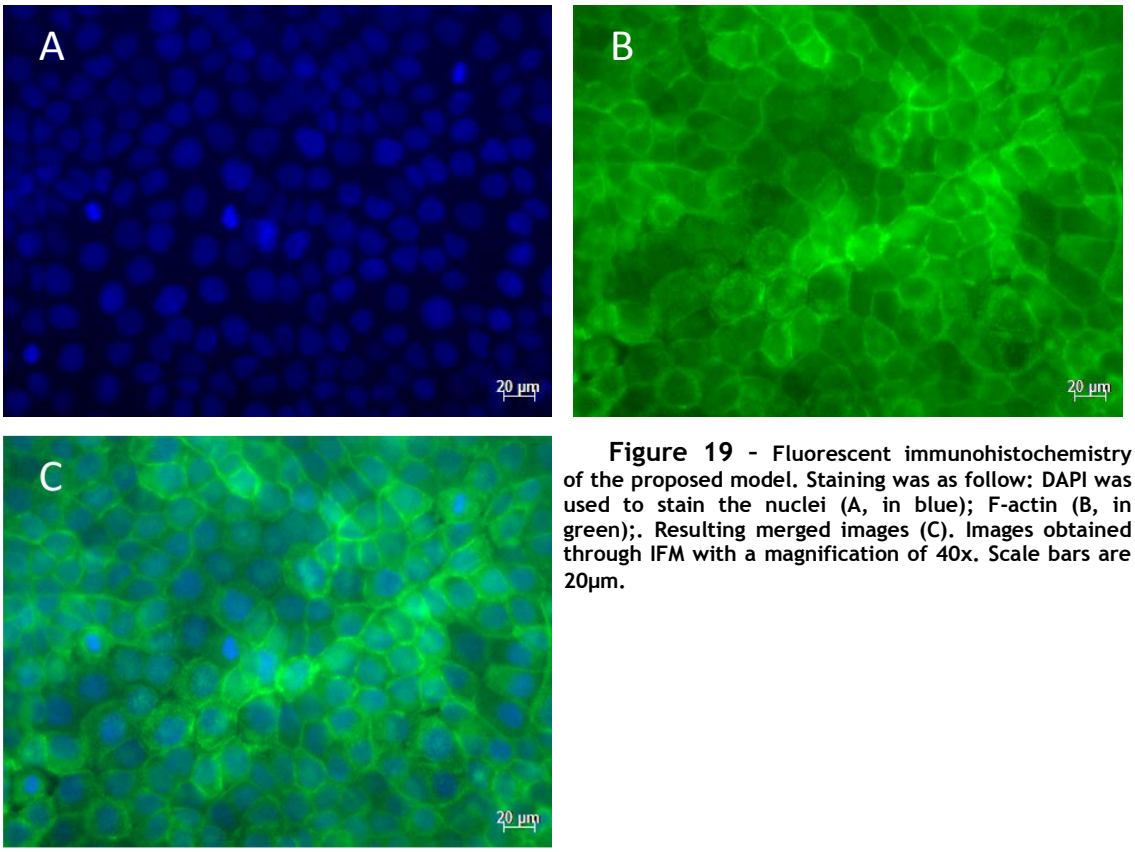

Figure 19 - Fluorescent immunohistochemistry of the proposed model. Staining was as follow: DAPI was used to stain the nuclei (A, in blue); F-actin (B, in green);. Resulting merged images (C). Images obtained through IFM with a magnification of 40x. Scale bars are 20µm.

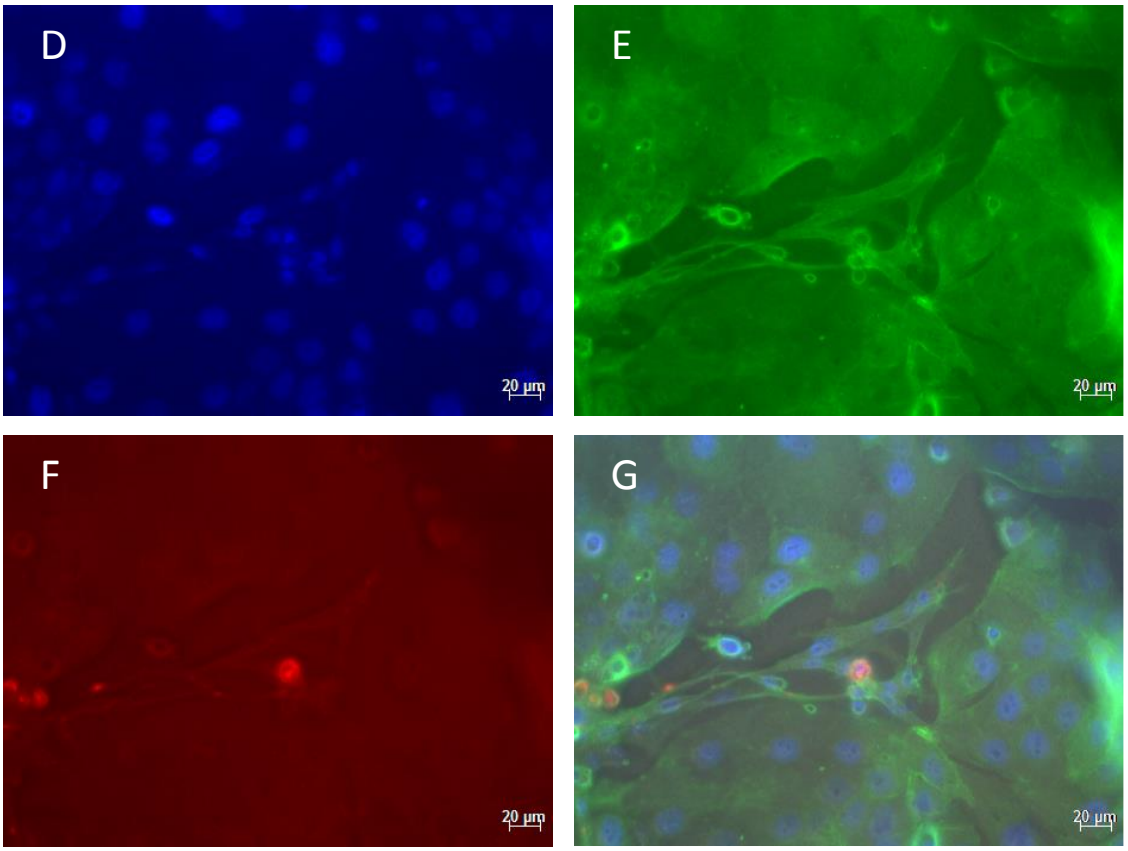

Figure 20 - Fluorescent immunohistochemistry of the proposed model. Staining was as follows: DAPI for the nuclei (D, in blue); F-actin (E, in green) vimentin (F, in red),). Resulting merged images (G). Images obtained through IFM with a magnification of 40x. Scale bars are 20µm.

Confocal Microscopy allowed for the confirmation of the structure observed for the "sandwich" model through IFM, as can be seen in Fig. 21. A tightly-knit epithelial layer can be seen on top, with fibroblasts underneath.

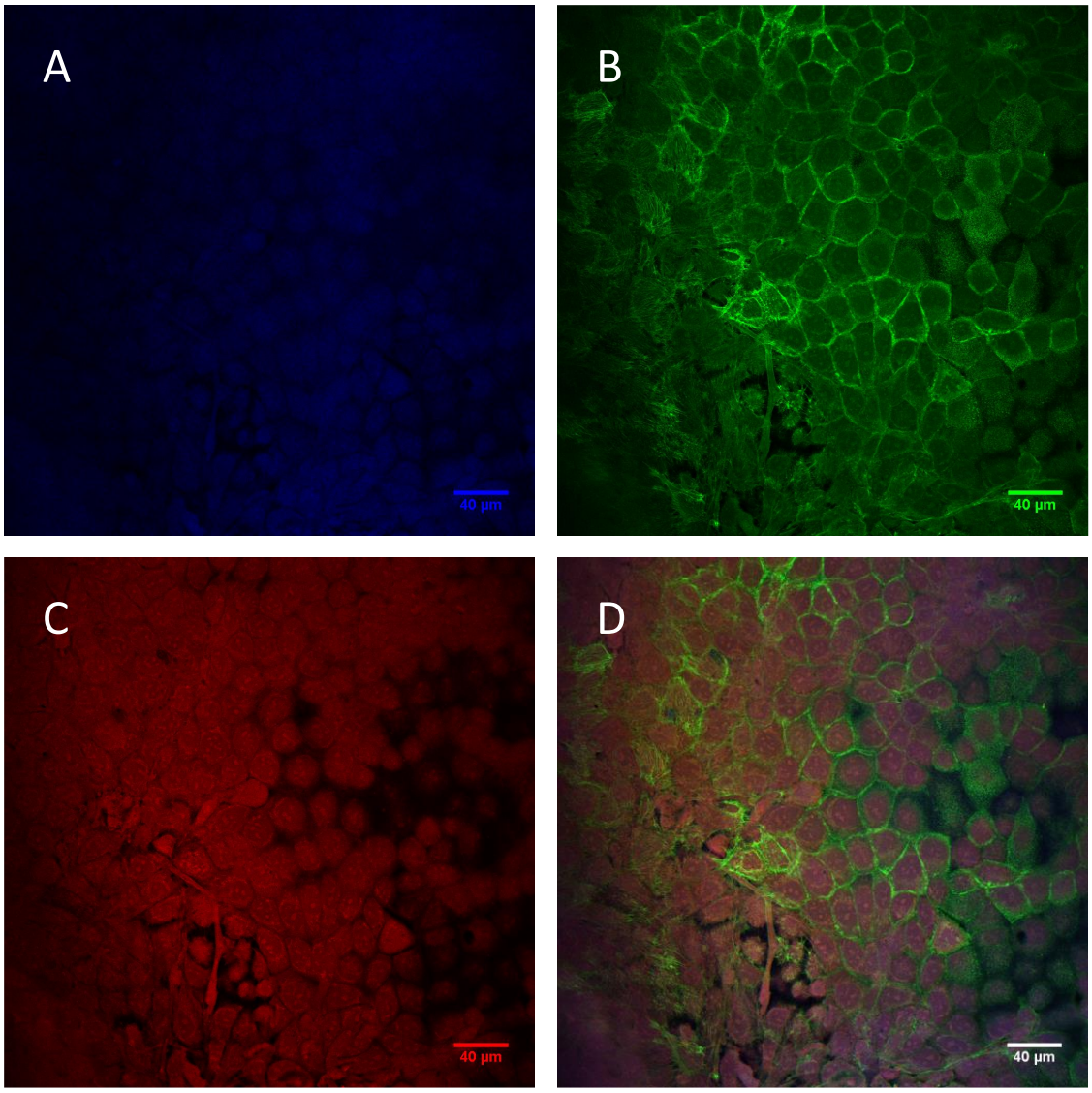

Figure 21 - Fluorescent immunohistochemistry of the proposed model. Staining was as follows: Dapi for the nuclei (A, in blue), F-actin (B, in green) and vimentin (C, in red). Resulting merged images (D). Images obtained through Confocal Microscopy with a magnification of 40x. Scale bars are 40µm.

Transmission Electron microscopy (TEM) was also performed on "sandwich" model with Matrigel as a means to assess the formation of tight junctions by the epithelial cells and the integrity of the barrier models overall, since this model proved to be the most reliable and similar to the *in vivo* morphological conditions, with other configurations presenting fractured epithelial cell layers. These images can be found in Figs. 22 and 23. It was possible to verify the formation of tight junctions between epithelial cells (more electrodense regions at the intersection of epithelial cells), which can be correlated with a higher barrier integrity [83], since they are responsible for the formation of a tightly-knit epithelium, which corroborates the results discussed above, in which the " sandwich" models presented a cohesive epithelium.

It could also be observed that the cells invaded the insert's pores, adhering to their walls on both sides of the filter. Since the cells can pass through the pores, it can be expected that some of them will be lost in the culture medium of the basolateral side. However, this should be a small percentage, since most of them will adhere to the apical side of the filter.

A staining with hematoxylin-eosin on a "sandwich model" without macrophages was also used to visualize the different cells layers, and their conformation within the proposed model. These images can be observed in Fig. 24.The hematoxylin-eosin staining confirmed

the architecture of the proposed models, since it can be observable that a layer of fibroblasts is adhered to the insert's filter, while the epithelial cells formed an epithelium on top of them, separated by extracellular matrix that is supposedly a mixture between matrigel or puramatrix (depending on the model in question) and the extracellular matrix secreted by the fibroblasts. It can be seen in the image that epithelial cells detached from the filter in some regions, and this was a recurrent problem resulting in decreased integrity and higher permeability. One possible explanation is that this happened due to the high difference in stiffness between the insert and paraffin, resulting in high mechanical sheer stress experienced upon slicing the thin paraffin sheets for the histological preparations, thus resulting in detachment of the cells from the membrane. Although different fixation and sectioning methods were employed, as well as longer fixation times, cells always detached in some regions. A possible solution for this would be to use larger transwells, so that the sheer stress inflicted upon the membrane was lower. Even longer fixation times could also improve the preservation of the membrane, thus preventing cell detachment.

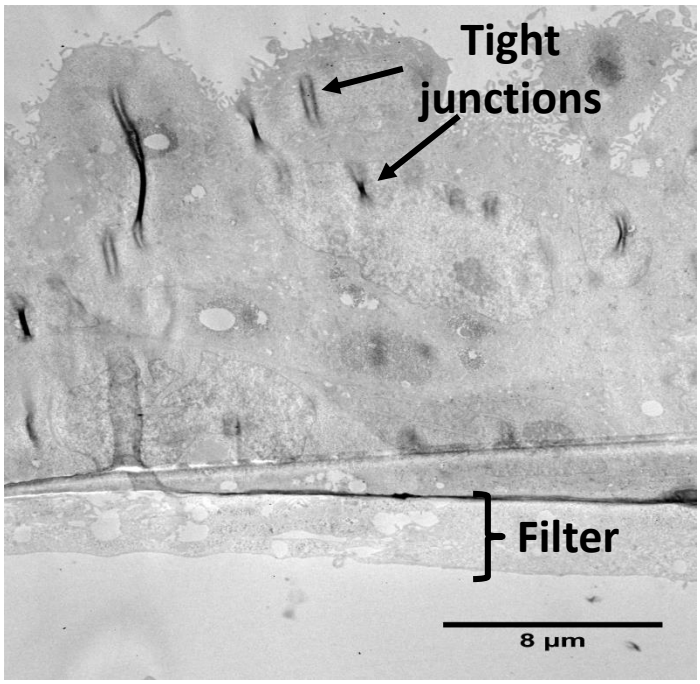

Figure 22 - TEM imaging of the proposed barrier models, evidencing the formation of an epithelial cell layer on top of the insert filter. The arrows represent tight junctions connecting epithelial cells, while the bracket marks the insert filter.

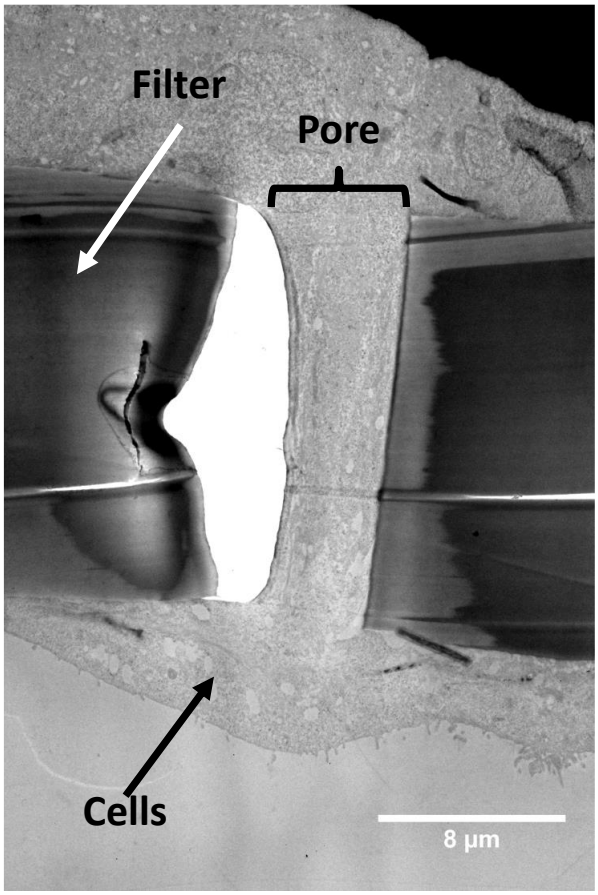

Figure 23 - TEM imaging of the proposed barrier models, with the filter's pores in evidence, represented by the bracket.

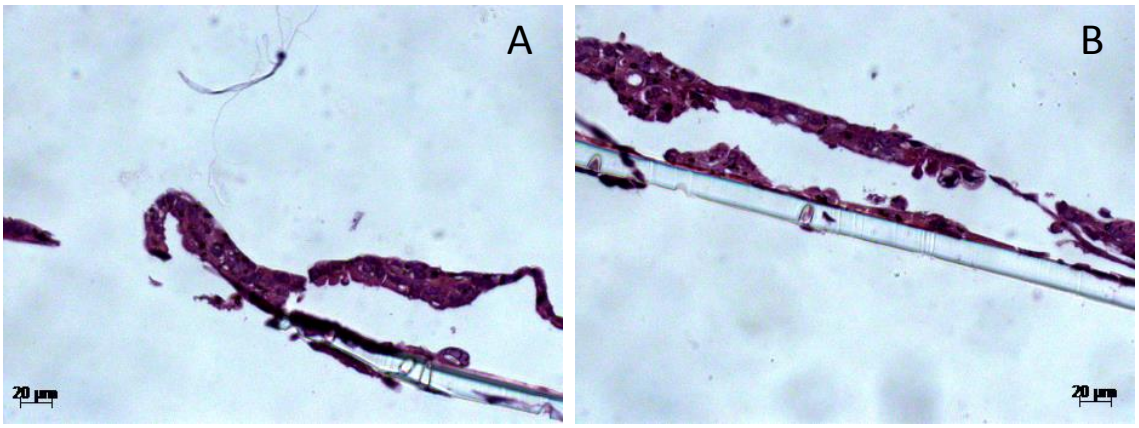

Figure 24 – A and B: Hematoxylin-eosin staining of the proposed barrier models, where the cytoplasm is stained in pink and the nuclei in blue.

Chapter 4

Conclusions

The aim of this project was to develop a cellularized artificial model of the gastric mucosa that could be used for either drug permeability testing or in toxicity assays, as a means to simulate the *in vivo* physiological and functional conditions of the mucosa, thus serving as a preliminary tool for drug development and testing.

In order to achieve this, model barriers were created by seeding fibroblasts and macrophages over Polyethylene terephthalate BD Falcon™ transwells inserts and coated with either BD™ Matrigel™ or BD™ PuraMatrix™, in order to simulate the *lamina propria* and then epithelial cells were seeded on top, to recreate the gastric epithelium.

TEER measurements were used to assess the barrier formation and its integrity and results showed that with an optimal combination of cell densities (5×10^3 NST20, 5×10^3 Macrophages and 5×10^4 MKN28), a stable and cohesive barrier could be achieved and maintained for up to a minimum of ten days after culture, while maintaining high TEER levels. These values are within the range found in similar models in the literature[5].

Based on the evolution of the TEER values over time, the best model configuration was found to be the "sandwich" model, in which the cells could grow and form an organized epithelium, while receiving molecular signals from the fibroblasts as well as spatial stimuli from the three-dimensional extracellular matrix. The use of fibroblasts and macrophages embedded on the extracellular matrix also provided interesting results, although not always being replicable, which can be due to the variable nature of the Matrigel. This poses a hurdle in replicating results, which is critical considering the applications of the proposed models for drug permeability and toxicity assays. Therefore, more reliable extracellular matrix replacements should be considered, such as alginate and pectin hydrogels [91, 92].

Another method of evaluating the integrity of the barrier models and their possible application as drug permeability models was assessing their apparent permeability, which yielded considerable results, namely after the introduction of macrophages, since the values of permeability obtained were even inferior to the ones obtained for epithelial monocultures, which produce a tightly-knit epithelium, with low permeability values, hence confirming the integrity of these models.

IFM and confocal microscopy also confirmed the formation of a cohesive epithelial layer, on top of a fibroblast layer, as intended. TEM imaging later supported this by showing the existence of tight junctions between the epithelial cells.

Considering all of these results, it is possible to conclude that the created models can be suitable for drug permeability testing and toxicity assays, since they model the gastric mucosa and mimic some of their functions, although further optimization and functional and morphological tests are required to confirm this.

In terms of future work, further optimization of the culture conditions would be necessary, in order to increase the reproducibility of the barrier models, as well as a more detailed morphological, structural and functional characterization, including immunohistochemistry to assess the presence of tight junction proteins, such as occludin and claudin-3; epithelial markers, such as E-cadherin and fibroblast and macrophage specific markers, such as vimentin and CD14, respectively.

It would also be interesting to study the different interactions between the different cells types that are part of the proposed models, namely the assessment of TGF-β levels, in order to understand the crosstalk between the cancer cells and the macrophages, as well as the differentiation of normal fibroblasts into cancer fibroblasts, through the assessment of α –smooth muscle actin.

Finally, in order to complete this model, a gastric mucus substitute should be added, either through cell induction (recurring to cell transfection or another gastric cell type which endogenously produce gastric mucus) or using a commercially available substitute. Indeed, a Fasted State Simulated Gastric Fluid (FaSSGF), commercially available, could be used at the top of the model, in order to mimic the real conditions found in the stomach, which take in consideration vital properties such as pH, osmolality, buffer capacity and surface tension of the gastric fluid.

References

1. Sarmento, B., et al., *Cell-based in vitro models for predicting drug permeability.* Expert Opin Drug Metab Toxicol, 2012. **8**(5): p. 607-21.
2. Araújo, F. and B. Sarmento, *Towards the characterization of an in vitro triple co-culture intestine cell model for permeability studies.* International Journal of Pharmaceutics, 2013. **458**(1): p. 128-134.
3. Antunes, F., et al., *Establishment of a triple co-culture in vitro cell models to study intestinal absorption of peptide drugs.* Eur J Pharm Biopharm, 2013. **83**(3): p. 427-35.
4. Hilgendorf, C., et al., *Caco-2 versus Caco-2/HT29-MTX co-cultured cell lines: permeabilities via diffusion, inside- and outside-directed carrier-mediated transport.* J Pharm Sci, 2000. **89**(1): p. 63-75.
5. Lemieux, M., et al., *The NCI-N87 cell line as a gastric epithelial barrier model for drug permeability assay.* Biochemical and Biophysical Research Communications, 2011. **412**(3): p. 429-434.
6. Talukder, R. and R. Fassihi, *Gastroretentive delivery systems: a mini review.* Drug Dev Ind Pharm, 2004. **30**(10): p. 1019-28.
7. Tavelin, S., et al., *Applications of Epithelial Cell Culture in Studies of Drug Transport*, in *Epithelial Cell Culture Protocols*, C. Wise, Editor. 2002, Humana Press. p. 233-272.
8. Xavier, J., *Study and Development of a Model for Mimicking the Gastric Mucosa*. 2012, FEUP/ICBAS -University of Porto.
9. Soybel, D.I., *Anatomy and Physiology of the Stomach.* Surgical Clinics of North America, 2005. **85**(5): p. 875-894.
10. Dimova, S., et al., *The use of human nasal in vitro cell systems during drug discovery and development.* Toxicol In Vitro, 2005. **19**(1): p. 107-22.
11. Olson, J.L., A. Atala, and J.J. Yoo, *Tissue engineering: current strategies and future directions.* Chonnam Med J, 2011. **47**(1): p. 1-13.
12. Esch, M.B., et al., *How multi-organ microdevices can help foster drug development.* Advanced Drug Delivery Reviews, (0).
13. Maemura, T., et al., *Assessment of tissue-engineered stomach derived from isolated epithelium organoid units.* Transplant Proc, 2004. **36**(5): p. 1595-9.
14. Maemura, T., M. Shin, and M. Kinoshita, *Tissue engineering of the stomach.* J Surg Res, 2013. **183**(1): p. 285-95.
15. Bitar, K.N. and E. Zakhem, *Tissue engineering and regenerative medicine as applied to the gastrointestinal tract.* Curr Opin Biotechnol, 2013. **24**(5): p. 909-15.
16. Polster, C.S., et al., *Use of artificial stomach-duodenum model for investigation of dosing fluid effect on clinical trial variability.* Mol Pharm, 2010. **7**(5): p. 1533-8.
17. Terano, A., et al., *Cell culture of rat gastric fundic mucosa.* Gastroenterology, 1982. **83**(6): p. 1280-91.
18. Matuoka, K., et al., *Cultured rabbit gastric epithelial cells producing prostaglandin I2.* Gastroenterology, 1983. **84**(3): p. 498-505.
19. Matsuda, K., et al., *Effects of growth factors and gut hormones on proliferation of primary cultured gastric mucous cells of guinea pig.* J Gastroenterol, 1996. **31**(4): p. 498-504.
20. Karam, S.M. and C.P. Leblond, *Identifying and counting epithelial cell types in the "corpus" of the mouse stomach.* Anat Rec, 1992. **232**(2): p. 231-46.
21. Chew, C.S., *Parietal cell culture: new models and directions.* Annu Rev Physiol, 1994. **56**: p. 445-61.
22. Matsumura, Y. and H. Maeda, *A new concept for macromolecular therapeutics in cancer chemotherapy: mechanism of tumoritropic accumulation of proteins and the antitumor agent smancs.* Cancer Res, 1986. **46**(12 Pt 1): p. 6387-92.

23. Jeong, C.G. and S.J. Hollister, *Mechanical, permeability, and degradation properties of 3D designed poly(1,8 octanediol-co-citrate) scaffolds for soft tissue engineering.* J Biomed Mater Res B Appl Biomater, 2010. **93**(1): p. 141-9.
24. Hong, Y., et al., *Tailoring the degradation kinetics of poly(ester carbonate urethane)urea thermoplastic elastomers for tissue engineering scaffolds.* Biomaterials, 2010. **31**(15): p. 4249-58.
25. Hori, Y., et al., *Experimental study on in situ tissue engineering of the stomach by an acellular collagen sponge scaffold graft.* ASAIO J, 2001. **47**(3): p. 206-10.
26. Araki, M., et al., *Development of a new tissue-engineered sheet for reconstruction of the stomach.* Artif Organs, 2009. **33**(10): p. 818-26.
27. Hori, Y., et al., *Functional analysis of the tissue-engineered stomach wall.* Artif Organs, 2002. **26**(10): p. 868-72.
28. Maemura, T., et al., *A tissue-engineered stomach as a replacement of the native stomach.* Transplantation, 2003. **76**(1): p. 61-5.
29. Sala, F.G., et al., *Tissue-engineered small intestine and stomach form from autologous tissue in a preclinical large animal model.* J Surg Res, 2009. **156**(2): p. 205-12.
30. Speer, A.L., et al., *Murine tissue-engineered stomach demonstrates epithelial differentiation.* J Surg Res, 2011. **171**(1): p. 6-14.
31. Maemura, T., et al., *Assessment of a tissue-engineered gastric wall patch in a rat model.* Artif Organs, 2012. **36**(4): p. 409-17.
32. Sarmento, B., et al., *Cell-based in vitro models for predicting drug permeability.* Expert Opinion on Drug Metabolism & Toxicology, 2012. **8**(5): p. 607-621.
33. Shah, A.K. and S.A. Agnihotri, *Recent advances and novel strategies in pre-clinical formulation development: an overview.* J Control Release, 2011. **156**(3): p. 281-96.
34. Bohets, H., et al., *Strategies for absorption screening in drug discovery and development.* Curr Top Med Chem, 2001. **1**(5): p. 367-83.
35. Rubas, W., et al., *Flux measurements across Caco-2 monolayers may predict transport in human large intestinal tissue.* J Pharm Sci, 1996. **85**(2): p. 165-9.
36. Mahler, G.J., M.L. Shuler, and R.P. Glahn, *Characterization of Caco-2 and HT29-MTX cocultures in an in vitro digestion/cell culture model used to predict iron bioavailability.* The Journal of Nutritional Biochemistry, 2009. **20**(7): p. 494-502.
37. Gupta, V., N. Doshi, and S. Mitragotri, *Permeation of insulin, calcitonin and exenatide across Caco-2 monolayers: measurement using a rapid, 3-day system.* PLoS One, 2013. **8**(2): p. e57136.
38. Antunes, F., et al., *Models to predict intestinal absorption of therapeutic peptides and proteins.* Curr Drug Metab, 2013. **14**(1): p. 4-20.
39. Lo, D., et al., *Cell culture modeling of specialized tissue: identification of genes expressed specifically by follicle-associated epithelium of Peyer's patch by expression profiling of Caco-2/Raji co-cultures.* Int Immunol, 2004. **16**(1): p. 91-9.
40. Lohikangas, L., et al., *Effects of a new lipid-based drug delivery system on the absorption of low molecular weight heparin (Fragmin) through monolayers of human intestinal epithelial Caco-2 cells and after rectal administration to rabbits.* European Journal of Pharmaceutical Sciences, 1994. **1**(6): p. 297-305.
41. Gorodeski, G.I., et al., *Human uterine cervical epithelial cells grown on permeable support--a new model for the study of differentiation.* Differentiation, 1994. **56**(1-2): p. 107-18.
42. Gorodeski, G.I. and J. Goldfarb, *Seminal fluid factor increases the resistance of the tight junctional complex of cultured human cervical epithelium CaSki cells.* Fertil Steril, 1998. **69**(2): p. 309-17.
43. Gorodeski, G.I., *The cultured human cervical epithelium: a new model for studying paracellular transport.* J Soc Gynecol Investig, 1996. **3**(5): p. 267-80.
44. Gorodeski, G.I., *Vaginal-cervical epithelial permeability decreases after menopause.* Fertil Steril, 2001. **76**(4): p. 753-61.
45. Ayehunie, S., et al., *Development of an in vitro alternative assay method for vaginal irritation.* Toxicology, 2011. **279**(1-3): p. 130-8.
46. Fatakdawala, H. and S.A. Uhland, *Hydrogen peroxide mediated transvaginal drug delivery.* Int J Pharm, 2011. **409**(1-2): p. 121-7.

47. Fuchs, S., et al., *Differentiation of human alveolar epithelial cells in primary culture: morphological characterization and synthesis of caveolin-1 and surfactant protein-C*. Cell Tissue Res, 2003. **311**(1): p. 31-45.
48. Forbes, B., et al., *The human bronchial epithelial cell line 16HBE14o- as a model system of the airways for studying drug transport*. Int J Pharm, 2003. **257**(1-2): p. 161-7.
49. Zhu, Y., A. Chidekel, and T.H. Shaffer, *Cultured human airway epithelial cells (calu-3): a model of human respiratory function, structure, and inflammatory responses.* Crit Care Res Pract, 2010. **2010**.
50. Stentebjerg-Andersen, A., et al., *Calu-3 cells grown under AIC and LCC conditions: implications for dipeptide uptake and transepithelial transport of substances.* Eur J Pharm Biopharm, 2011. **78**(1): p. 19-26.
51. Grainger, C.I., et al., *Culture of Calu-3 cells at the air interface provides a representative model of the airway epithelial barrier*. Pharm Res, 2006. **23**(7): p. 1482-90.
52. Wang, Z.Y., Y. Zhang, and Q. Zhang, *[Transport of proteins and peptides across human cultured alveolar A549 cell monolayers].* Yao Xue Xue Bao, 2004. **39**(5): p. 392-5.
53. Forbes, B. and C. Ehrhardt, *Human respiratory epithelial cell culture for drug delivery applications.* Eur J Pharm Biopharm, 2005. **60**(2): p. 193-205.
54. Rothen-Rutishauser, B.M., S.G. Kiama, and P. Gehr, *A three-dimensional cellular model of the human respiratory tract to study the interaction with particles.* Am J Respir Cell Mol Biol, 2005. **32**(4): p. 281-9.
55. Lehmann, A.D., et al., *An in vitro triple cell co-culture model with primary cells mimicking the human alveolar epithelial barrier.* Eur J Pharm Biopharm, 2011. **77**(3): p. 398-406.
56. Hermanns, M.I., et al., *Lung epithelial cell lines in coculture with human pulmonary microvascular endothelial cells: development of an alveolo-capillary barrier in vitro.* Lab Invest, 2004. **84**(6): p. 736-52.
57. Agu, R.U., et al., *Nasal absorption enhancement strategies for therapeutic peptides: an in vitro study using cultured human nasal epithelium.* Int J Pharm, 2002. **237**(1-2): p. 179-91.
58. Wengst, A. and S. Reichl, *RPMI 2650 epithelial model and three-dimensional reconstructed human nasal mucosa as in vitro models for nasal permeation studies.* European Journal of Pharmaceutics and Biopharmaceutics, 2010. **74**(2): p. 290-297.
59. Toropainen, E., et al., *Culture model of human corneal epithelium for prediction of ocular drug absorption.* Invest Ophthalmol Vis Sci, 2001. **42**(12): p. 2942-8.
60. Enriquez-de-Salamanca, A., et al., *Cytokine responses by conjunctival epithelial cells: an in vitro model of ocular inflammation.* Cytokine, 2008. **44**(1): p. 160-7.
61. Kudela, P., et al., *Bacterial Ghosts as antigen and drug delivery system for ocular surface diseases: Effective internalization of Bacterial Ghosts by human conjunctival epithelial cells.* J Biotechnol, 2011. **153**(3-4): p. 167-75.
62. Hornof, M., E. Toropainen, and A. Urtti, *Cell culture models of the ocular barriers.* Eur J Pharm Biopharm, 2005. **60**(2): p. 207-25.
63. Barar, J., et al., *Ocular Drug Delivery; Impact of in vitro Cell Culture Models.* J Ophthalmic Vis Res, 2009. **4**(4): p. 238-52.
64. Schaefer, U.F., et al., *Models for Skin Absorption and Skin Toxicity Testing*, in *Drug Absorption Studies*, C. Ehrhardt and K.-J. Kim, Editors. 2008, Springer US. p. 3-33.
65. Hu, T., et al., *Dermal penetration and metabolism of p-aminophenol and p-phenylenediamine: application of the EpiDerm human reconstructed epidermis model*. Toxicol Lett, 2009. **188**(2): p. 119-29.
66. Netzlaff, F., et al., *The human epidermis models EpiSkin, SkinEthic and EpiDerm: an evaluation of morphology and their suitability for testing phototoxicity, irritancy, corrosivity, and substance transport*. Eur J Pharm Biopharm, 2005. **60**(2): p. 167-78.
67. Gabbanini, S., et al., *Analysis of in vitro release through reconstructed human epidermis and synthetic membranes of multi-vitamins from cosmetic formulations.* J Pharm Biomed Anal, 2010. **52**(4): p. 461-7.

68. Chailler, P. and D. Menard, *Establishment of human gastric epithelial (HGE) cell lines exhibiting barrier function, progenitor, and prezymogenic characteristics.* J Cell Physiol, 2005. **202**(1): p. 263-74.
69. Basque, J.R., et al., *Gastric cancer cell lines as models to study human digestive functions.* J Cell Biochem, 2001. **81**(2): p. 241-51.
70. Motoyama, T., H. Hojo, and H. Watanabe, *COMPARISON OF SEVEN CELL LINES DERIVED FROM HUMAN GASTRIC CARCINOMAS.* Pathology International, 1986. **36**(1): p. 65-83.
71. Wroblewski, L.E., et al., *Helicobacter pylori Dysregulation of Gastric Epithelial Tight Junctions by Urease-Mediated Myosin II Activation.* Gastroenterology, 2009. **136**(1): p. 236-246.
72. Turner, J.R., *Molecular basis of epithelial barrier regulation: from basic mechanisms to clinical application.* Am J Pathol, 2006. **169**(6): p. 1901-9.
73. Tsuchiya, S., et al., *Establishment and characterization of a human acute monocytic leukemia cell line (THP-1).* Int J Cancer, 1980. **26**(2): p. 171-6.
74. Tominaga, T., et al., *Establishment of an activated macrophage cell line, A-THP-1, and its properties.* Tohoku J Exp Med, 1998. **186**(2): p. 99-119.
75. da Cunha, C.B., et al., *De novo expression of CD44 variants in sporadic and hereditary gastric cancer.* Lab Invest, 2010. **90**(11): p. 1604-1614.
76. Jiang, X.H., et al., *Functional p53 is required for triptolide-induced apoptosis and AP-1 and nuclear factor-kappaB activation in gastric cancer cells.* Oncogene, 2001. **20**(55): p. 8009-18.
77. Daigneault, M., et al., *The Identification of Markers of Macrophage Differentiation in PMA-Stimulated THP-1 Cells and Monocyte-Derived Macrophages.* PLoS ONE, 2010. **5**(1): p. e8668.
78. Fonte, P., et al., *Chitosan-coated solid lipid nanoparticles enhance the oral absorption of insulin.* Drug Delivery and Translational Research, 2011. **1**(4): p. 299-308.
79. Vllasaliu, D., et al., *Tight junction modulation by chitosan nanoparticles: comparison with chitosan solution.* Int J Pharm, 2010. **400**(1-2): p. 183-93.
80. Pitkänen, L., et al., *Permeability of Retinal Pigment Epithelium: Effects of Permeant Molecular Weight and Lipophilicity.* Investigative Ophthalmology & Visual Science, 2005. **46**(2): p. 641-646.
81. P. Nejdfors, M.E., B. Jeppsson, B. R. Weström, *Mucosal in Vitro Permeability in the Intestinal Tract of the Pig, the Rat, and Man: Species- and Region-Related Differences.* Scandinavian Journal of Gastroenterology, 2000. **35**(5): p. 501-507.
82. Steed, E., M.S. Balda, and K. Matter, *Dynamics and functions of tight junctions.* Trends in Cell Biology, 2010. **20**(3): p. 142-149.
83. Van Itallie, C.M. and J.M. Anderson, *Claudins and epithelial paracellular transport.* Annu Rev Physiol, 2006. **68**: p. 403-29.
84. Mukherjee, T., et al., *Transepithelial Electrical Resistance is Not a Reliable Measurement of the Caco-2 Monolayer Integrity in Transwell.* Drug Delivery, 2004. **11**(1): p. 11-18.
85. Hughes, C.S., L.M. Postovit, and G.A. Lajoie, *Matrigel: a complex protein mixture required for optimal growth of cell culture.* Proteomics, 2010. **10**(9): p. 1886-90.
86. Maia, F.R., et al., *Effect of cell density on mesenchymal stem cells aggregation in RGD-alginate 3D matrices under osteoinductive conditions.* Macromol Biosci, 2014. **14**(6): p. 759-71.
87. Gelain, F., A. Horii, and S. Zhang, *Designer self-assembling peptide scaffolds for 3-d tissue cell cultures and regenerative medicine.* Macromol Biosci, 2007. **7**(5): p. 544-51.
88. dos Santos, T., et al., *Quantitative Assessment of the Comparative Nanoparticle-Uptake Efficiency of a Range of Cell Lines.* Small, 2011. **7**(23): p. 3341-3349.
89. Goodpaster, T., et al., *An Immunohistochemical Method for Identifying Fibroblasts in Formalin-fixed, Paraffin-embedded Tissue.* Journal of Histochemistry & Cytochemistry, 2008. **56**(4): p. 347-358.
90. Soybel, D.I., *Anatomy and physiology of the stomach.* Surg Clin North Am, 2005. **85**(5): p. 875-94, v.

91. Bidarra, S.J., C.C. Barrias, and P.L. Granja, *Injectable alginate hydrogels for cell delivery in tissue engineering.* Acta Biomater, 2014. **10**(4): p. 1646-62.
92. Maia, F.R., et al., *Matrix-driven formation of mesenchymal stem cell-extracellular matrix microtissues on soft alginate hydrogels.* Acta Biomater, 2014. **10**(7): p. 3197-208.